

SUMMARY OF CHANGES

The manuscript has been revised according to the reviewers' comments. The detailed modifications are listed as follows:

- 1 The **abstract** has been revised to clarify the statement on the new universality class, explicitly emphasizing the significant impact of the newly identified universality class on Gross-Neveu criticality.

2 Changes in the main text:

- (1) In the **Introduction** section, on page 1, 1st paragraph, right column, the redundant statement about the importance of the problem has been removed.
- (2) In the **Introduction** section, on page 1, 2nd paragraph, right column, we explicitly state that our method is used to unveil the ground-state phase diagram.
- (3) In the **Introduction** section, on page 2, 1st paragraph, left column, we explicitly state that the discovered phase transition defines an unconventional Gross-Neveu universality class.
- (4) In the **Theoretical framework** section, on page 2, 2nd paragraph, left column, we add that the universal scaling form is satisfied after a transient nonuniversal time scale.
- (5) In the **Single-Dirac-fermion Hubbard model** section, on page 3, 1st paragraph, left column, we add that the lattice geometry is square.
- (6) In the **Single-Dirac-fermion Hubbard model** section, on page 3, 2nd paragraph, right column, the entire paragraph has been rewritten to analyze the accuracy of our method. The choice of τL^{-z} and the selection of initial states are also discussed.
- (7) In the **Spinless t - V model** section, on page 4, 2nd paragraph, left column, we strengthen the emphasis that different choices of initial states provide a self-consistent benchmark.
- (8) In the **SU(3) Hubbard model** section, on page 4, 4th paragraph, right column, we explicitly state that the order parameter has SU(3) symmetry, which is different from the O(N) order parameters in previous Gross-Neveu transitions.
- (9) In the **SU(3) Hubbard model** section, on page 5, 2nd paragraph, left column, we state that the newly discovered universality class is different from conventional Gross-Neveu universality classes.
- (10) In the **Concluding remarks** section, on page 5, 3rd paragraph, left column, we emphasize that our framework can reveal ground-state properties and quantum phases, distinguish first-order from continuous phase transitions, and we also highlight the accuracy benchmarks of our method.
- (11) In the **Concluding remarks** section, on page 5, 2nd paragraph, right column, the entire paragraph has been rewritten to fully discuss the significance of our solution to the SU(3) Hubbard model.
- (12) In the **Concluding remarks** section, on page 5, 3rd paragraph, right column, the entire paragraph has been rewritten to fully discuss the applicability and future prospects of our new framework.

3 Changes in figures:

- (1) In the insets of Figure 1a, legends have been added to avoid confusion.
- (2) In the captions of Figures 1, 2, 3, $z = 1$ has been specified.
- (3) In Figures 1c, 1d, 1e, 2b, 2c, 2d, 3c, 3d, 3e, additional data points have been computed, more than doubling the effective data used for the data collapse. Dashed lines have been added to indicate the boundaries of the nonequilibrium scaling region. The χ^2_ν values have been included in the captions to show the quality of the collapse.

4 Changes in Supplementary Materials:

- (1) Section I-D adds an example illustrating the application of our short-time method to first-order phase transitions.

- (2) Section II-B provides detailed procedures and technical steps for self-consistently assessing the accuracy of results within the short-time framework.
- (3) Section IV-D has been completely rewritten to fully discuss the newly identified universality class.
- (4) Figures S5b, S5d, S10b, S10d, S15b, S15d, S16b, S16d now include dashed lines indicating the nonequilibrium scaling range.

Some other minor changes to correct typos are not listed.

RESPONSE TO REVIEWER 1

Comment:

This is a well written and important paper proposing the use of the evolution of correlation functions in imaginary time to obtain the critical properties of correlated fermion models, including the single Dirac fermion Hubbard model, the spinless t - V model, and the SU(3) staggered flux Hubbard model. The former have known critical points, allowing the new method to be benchmarked. The latter is less well explored, so that new physics can be uncovered, making the manuscript more than an “algorithm paper”.

Because relatively small tau are required, the sign problem is less severe, and larger space-time lattices are accessible. Both of these allow a more robust analysis of the critical properties.

Reply:

We sincerely thank the reviewer for the very positive evaluation of our work. The reviewer’s detailed suggestions on each round have greatly helped us to improve the quality of the manuscript, for which we are truly grateful.

Comment:

One of the central points of the paper is that the physics can be revealed at such short imaginary times (high temperature T). Figure 1, panels b,c are for $\tau L^{-z} = 0.3$, that is $\tau/2 \sim 3$ for $L = 20$. ($\tau/2$ is the projection distance in Equation S1.) In the usual fermion Hubbard model $\beta = 3$ is not low enough T to see magnetic correlations develop. The SM provide a detailed analysis of the hierarchy of scales of τ which make the method work. I believe a somewhat more detailed synopsis of this discussion would be useful in the main body of the paper. As it is, the reader might be left to wonder what $\tau = 3$ is long enough.

Reply:

We thank the reviewer for the suggestion. In the revised manuscript, we have added a more detailed explanation in the main text regarding the rationale for choosing τL^{-z} [See Change 2(6)]. In addition, we further provide in the SM Sec. II-B a quantitative analysis of the nonequilibrium scaling regime [See Change 4(2)], which complements the discussion of the hierarchy of scales of τ . From the technical perspective, our self-consistent criterion for whether τ is sufficiently long is based on checking the convergence of the results when varying τL^{-z} , as well as verifying the consistency of the results obtained from different initial states.

For example, consider the results in Figs. 1b-1c of the main text, where using the DSM initial state we obtained $U_c = 7.220(37)$ at $\tau L^{-z} = 0.3$. In this revision, we have supplemented the data by extending τL^{-z} to 0.5 (see SM Figs. S3c-S3d), obtaining $U_c = 7.225(34)$, which is consistent with the result at $\tau L^{-z} = 0.3$ within the error bars. This demonstrates that our imaginary-time evolution has already entered the nonequilibrium scaling region and that the value of the critical point has converged and no longer changes with τL^{-z} . More importantly, in SM Figs. S3a-S3b we also consider the FM initial state and obtain $U_c = 7.214(44)$ at $\tau L^{-z} = 0.5$, which is again consistent with the DSM initial state result within the error bars. Moreover, the additional analysis of the scaling-collapse details for the critical exponents (see SM Fig. S6) provides a more direct and quantitative demonstration that $\tau L^{-z} = 0.3$ is already sufficient for the critical exponents obtained from different initial states to converge to the same value. This flexibility in the choice of initial states, together with the ability of self-consistency checks, provides a significant advantage of the nonequilibrium approach compared with finite-temperature scaling or finite-size scaling in conventional equilibrium approaches.

Comment:

I am confused by one aspect of the inset to Figure 1a. The caption says the red dashed line is for $\tau = 0.3L^z$, but the horizontal axis is tau. Does this mean the curve is for different lattice sizes L ?

Reply:

We thank the reviewer for pointing out this issue. The different curves in Fig. 1a indeed correspond to different L ,

consistent with the legend in Fig. 1e. To avoid possible confusion, we have added a legend to Fig. 1a in the revised version [See Change 3(1)].

Comment:

In discussing the spinless t - V model the initial state (CDW) is specified. I did not see analogous information for the SLAC fermion Hubbard model. This might be related to the point above concerning why $\tau/2 = 3$ is large enough. Maybe some “good starting point” (initial state) was chosen which was already close to the ground state so that $\tau/2 = 3$ is enough to get the rest of the way there?

Reply:

We thank the reviewer for this helpful comment. In fact, in SM Sec. II-B we have already provided the results for the SLAC fermion Hubbard model starting from a fully ordered ferromagnetic (FM) initial state, as a consistency check against the results in the main text obtained from the Dirac semimetal (DSM) initial state. The two sets of results agree. This important cross-check had not been mentioned in the main text, and we have now added it in the revised version [See Change 2(6)]. The consistency of the critical point and exponents obtained from different initial states is indeed an essential criterion for judging whether τ is sufficiently long. In addition, the reviewer’s conjecture is correct: the time to enter the nonequilibrium scaling regime differs for different initial states, and so does the timescale of their relaxation toward the ground state. Our tests show that for the FM initial state, convergence requires $\tau = 0.5L^z$, which is somewhat longer than in the DSM case. Moreover, the FM initial state suffers from a more severe sign problem, leading to larger statistical errors.

Comment:

It might be useful to specify $z = 1$ in the Figure captions. $z = 1$ is stated in the paper text, eg page 2 col 2 and page 3 col 1, but putting it in the captions would make it easy to find for the readers who focus on the data initially.

Reply:

We thank the reviewer for the suggestion. In the revised version, we have specified $z = 1$ in the figure captions to assist readers who focus on the data [See Change 3(2)].

Comment:

It would be useful to specify the lattice geometry for the single Dirac fermion Hubbard model (equation 2), as is done in for the spinless t - V model (equation 3, honeycomb).

Reply:

We thank the reviewer for the suggestion. In the revised manuscript, we have specified that the single-Dirac-fermion Hubbard model is defined on the square lattice [See Change 2(5)].

Comment:

This is an interesting paper proposing a new way around a major bottleneck in an important field. I support its acceptance in Scienc Advances.

Reply:

We sincerely thank the reviewer for supporting our work. We are also very grateful for the many constructive suggestions and insightful comments provided throughout the review process.

Comment:

Minor typographical points:

[01] In abstract, “nonequilibrium critical dynamic” → “nonequilibrium critical dynamics”.

[01] There are various places where one might insert prepositions, e.g. in the introduction, “mitigate sign problem” → “mitigate the sign problem”; “understanding of QCP” → ”understanding of the QCP”, and

“preempt sign problem” → “preempt the sign problem”. The authors/editors should look into these throughout the manuscript.

[02] The authors should consider removing the sentence ”Developing a generic unbiased ...” They have already established the importance of what they are attempting.

[03] There is a mix of boldface “i” and un-boldface “i” in Equation 2. (Elsewhere in the manuscript and SM, most of the site indices are not bold-face.)

Reply:

We thank the reviewer for these careful notes. We have corrected these typographical issues and carefully checked the entire manuscript to revise similar problems.

RESPONSE TO REVIEWER 2

Comment:

The present version of the manuscript does not improve the previous one and does not meet the general criteria for Science Advances.

Reply:

We sincerely thank the reviewer for carefully reviewing our manuscript again. In the previous revision, we responded seriously to the reviewer's concerns and made targeted modifications. In particular, regarding the "really important open question" raised by the reviewer:

Indeed, it could give some insight to determine (with what accuracy, in more complicated cases?) critical exponents once we know that there a QCP separating two phases, but it does not give any new input to determine the actual phase diagram of a strongly-correlated system. The latter one is a really important open question, which deserves high visibility.

We explicitly explained that our new framework is specifically suitable to determine the phase diagram of strongly correlated systems with sign problems, including the identification of various phases and phase boundaries, without requiring any prior knowledge of the QCP. We demonstrate this capability in the SU(3) Hubbard model. By identifying the unique channel in which the correlation-length ratio exhibits a crossing (while no crossing appears in other channels), we correctly determine the λ_8 antiferromagnetic ordered phase in the ground-state phase diagram and accurately locate the phase boundary between the Dirac semimetal and the λ_8 antiferromagnetic phase for the first time, without requiring any prior knowledge. The most important significance of our method lies in enabling unbiased solutions for a broad class of systems with sign problem that were previously inaccessible to QMC, thereby greatly expanding the scope of theoretical physics research, rather than merely improving the accuracy of calculating critical exponents. At that revision, we deliberately restructured the discussion section of the main text and added three sections in the Supplementary Materials (SM I-D, SM I-E, SM II-C) to elaborate on how our method can determine the QCP and phase diagram of an unknown system without any prior information, and to clarify to what extent our approach extends the research frontier of QMC.

In this round of revision, we have further improved our framework based on the reviewer's valuable feedback. In particular, we have supplemented quantitative and comprehensive calculations and analyses addressing the reviewer's specific concerns about the accuracy of critical exponents and the identification of first-order phase transitions. These new results once again demonstrate that our nonequilibrium short-time framework is capable of precisely determining the phase diagrams and critical properties of strongly correlated systems.

The reviewer's insight into the general interest has also encouraged us to analyze and discuss more deeply our new findings in the SU(3) Hubbard model. As Reviewer 1 highlighted, the SU(3) staggered flux Hubbard model represents an underexplored frontier where new physics can emerge, elevating our manuscript beyond a mere algorithm paper. Our study unequivocally achieves this, revealing fundamental new physics of broad interest, as will be demonstrated in the subsequent answers. The SU(3) Hubbard model, a critical example in the strongly correlated physics, cold atom and even high-energy physics, has now been solved with numerical exactness for the first time, thanks to our framework preempting the sign problem. Beyond this, the novel phase transition we discovered introduces the first non-trivial universality class within the Gross-Neveu family that deviates from a classical $O(N)$ order structure, which has attracted intensive investigations in last two decades. This significantly extends the Gross-Neveu universality classes, revealing intrinsic features of Dirac fermions, opening a new chapter in the theory of quantum phase transition and statistics physics. These breakthroughs, in both the SU(3) Hubbard model and in overcoming the sign problem, possess broad appeal across strongly correlated physics, statistical mechanics, cold atom physics, high-energy physics, and quantum chemistry. They clearly demonstrate that our new framework opens a promising new avenue for quantum many-body physics studies, continuing to resolve more long-standing challenges across diverse fields.

We are very grateful for the reviewer taking the time to read our detailed responses and revisions below. With the reviewer's help, the quality of our manuscript has been significantly improved, and we believe that this latest revised

version meets the standards of *Science Advances*. We look forward to the reviewer's feedback.

Comment:

The authors present a couple of benchmarks on “relatively simple” models, where the results agree with what is already known. It is not clear what is the actual accuracy of these results, e.g., how much the critical exponents will change by choosing a different scaling for τ/L . The data collapsing in Figs. 1e and 2c is not completely satisfactory. What is the impact on the errorbar on the critical indices?

Reply:

We sincerely thank the reviewer for the constructive comments on the accuracy of our method, which indeed help us improve the rigor and completeness of the manuscript in terms of technical details.

Regarding the accuracy of the critical exponents, in addition to the benchmarks against previous results, we have supplemented the manuscript with a more thorough, detailed, and self-consistent analysis and clarification in this reply and the updated manuscript [See Changes 2(6), 2(7), 2(10), 4(2)]. Indeed, as the reviewer is concerned, for too small values of τL^{-z} , the system remains too close to the initial state, outside the nonequilibrium scaling region governed by the critical point, and the scaling relations no longer hold. In this case, choosing a different scaling for τL^{-z} will indeed change the extracted critical exponents. Once τL^{-z} is sufficiently large and the system has entered the nonequilibrium scaling region, the fitted critical exponents become independent of τL^{-z} .

In practice, we apply this criterion to precisely determine the critical exponents and delineate the non-equilibrium scaling region. During data collapse analysis, we systematically vary the lower bound of τL^{-z} , denoted as $(\tau L^{-z})_{\min}$, and examine how the fitted critical exponents vary with $(\tau L^{-z})_{\min}$, as shown in Figs. R1a and Figs. R1e. As $(\tau L^{-z})_{\min}$ for the data collapse increases, the fitted critical exponents gradually converge and, within the resolution of the error bars, no longer change with $(\tau L^{-z})_{\min}$. Moreover, the critical exponents obtained from nonequilibrium processes starting from different initial states converge to the same results within the error bars—this is the hallmark of having entered the nonequilibrium scaling region.

For example, regarding the critical exponent η_ϕ in the single-Dirac-fermion Hubbard model, Fig. R1a shows that η_ϕ converges once $(\tau L^{-z})_{\min} > 0.25$, and the results obtained from nonequilibrium processes starting from different initial states are consistent. We use the reduced χ^2_ν to assess the quality of the data collapse:

$$\chi^2_\nu = \frac{1}{\nu} \sum_{i=1}^N \sum_{L=1}^{N_L} \frac{(y_{iL} - \mu_i)^2}{\Delta y_{iL}^2}. \quad (\text{R1})$$

For the rescaled curves corresponding to different system sizes L (N_L curves in total), we perform linear interpolation and then uniformly sample $N = 50$ values of τL^{-z} to obtain the curve ordinates y_{iL} and their uncertainties Δy_{iL} . We then compute the weighted mean $\mu_i = \sum_L w_{iL} y_{iL} / \sum_L w_{iL}$ with weights $w_{iL} = 1/\Delta y_{iL}^2$. The degrees of freedom for the reduced chi-square are $\nu = N(N_L - 1)$. As shown in Fig. R1b, when $(\tau L^{-z})_{\min}$ is very small, $\chi^2_\nu \gg 1$, indicating very poor collapse quality and that the scaling form cannot describe such short $(\tau L^{-z})_{\min}$. As $(\tau L^{-z})_{\min}$ increases, χ^2_ν decreases. Around $0.2 < (\tau L^{-z})_{\min} < 0.35$, χ^2_ν approaches 1, where the quality of the data collapse is optimal. Further increasing $(\tau L^{-z})_{\min}$ leads to $\chi^2_\nu < 1$, which implies overfitting. This occurs because data points at larger τL^{-z} suffer from more severe sign problems and thus have larger errors, exceeding the resolution of the collapse. Taking into account the convergence behavior in Fig. R1a, the consistency between results from different initial states, and the collapse quality shown in Fig. R1b, we finally choose $(\tau L^{-z})_{\min} = 0.3$ as the lower bound for τL^{-z} in the data collapse analysis of the structure factor S for the single-Dirac-fermion Hubbard model. We evaluate the uncertainty of the critical exponent using a resampling technique. As shown in Fig. R1c, we randomly perturb the data of the structure factor S according to the size of the error bars of the original data and then perform the data collapse analysis again to extract η_ϕ . Figure R1c presents the histogram of η_ϕ obtained from 1000 resamplings, showing consistent results between the DSM and FM initial states. By fitting the histogram with a Gaussian distribution, we obtain the critical exponent as $\eta_\phi = 0.36(3)$ for the DSM initial state and $\eta_\phi = 0.35(3)$ for the FM initial state. Figure R1d displays the rescaled data collapse using these results. The black dashed line marks $\tau L^{-z} = 0.3$, with the region to the right included in the scaling analysis, where curves of different system sizes collapse perfectly. The region to the left of the dashed line is outside the scaling regime, and the deviations from scaling can be seen from the degree of non-overlap between curves. Figure R1d also shows that the system has not yet evolved to equilibrium (which typically requires

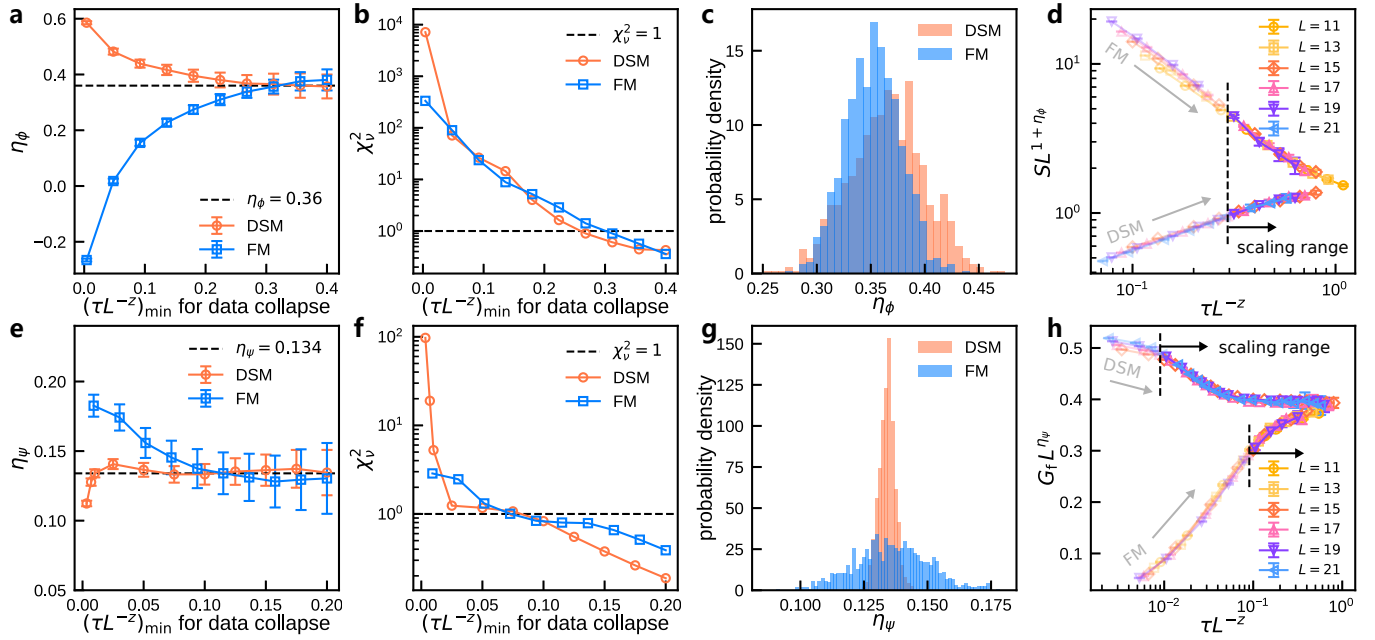


FIG. R1. **Technical details of determining the critical exponents in the single-Dirac-fermion Hubbard model via data collapse.** **a–d**, Determination of the critical exponent η_ϕ . **a**, Fitted values of η_ϕ versus the lower bound $(\tau L^{-z})_{\min}$ used in the data collapse analysis. The legend “DSM” denotes data collapse performed with the Dirac semi-metal initial state (the lower set of curves in **d**); the legend “FM” denotes data collapse performed with the ferromagnetic initial state (the upper set of curves in **d**). **b**, Reduced χ^2_ν of the data collapse versus $(\tau L^{-z})_{\min}$. **c**, Distribution of the fitted η_ϕ obtained from 1000 resamplings with $(\tau L^{-z})_{\min} = 0.3$. The results are $\eta_\phi = 0.36(3)$ with the DSM initial state and $\eta_\phi = 0.35(3)$ with the FM initial state. **d**, Scaling collapse of curves of the structure factor S_{FM} versus rescaled τ at U_c . **e–h**, Determination of the critical exponent η_ψ . **e**, Fitted values of η_ψ versus $(\tau L^{-z})_{\min}$. The legend “DSM” denotes data collapse performed with the DSM initial state (the upper set of curves in **h**); the legend “FM” denotes data collapse performed with the FM initial state (the lower set of curves in **h**). **f**, Reduced χ^2_ν of the data collapse versus $(\tau L^{-z})_{\min}$. **g**, Distribution of the fitted η_ψ obtained from 1000 resamplings with $(\tau L^{-z})_{\min} = 0.01$ for the DSM initial state and $(\tau L^{-z})_{\min} = 0.1$ for the FM initial state. The results are $\eta_\psi = 0.134(3)$ for the DSM initial state and $\eta_\psi = 0.136(14)$ for the FM initial state. **h**, Scaling collapse of curves of the fermion correlation G_f versus rescaled τ at U_c .

$\tau L^{-z} \sim 2\text{--}3$). Nevertheless, we are able to determine the accurate ground-state critical exponents from nonequilibrium data. Comparing Figs. R1a and R1d, for the system sizes we studied, the τL^{-z} needed for the convergence of η_ϕ is about one order of magnitude smaller than that required for the convergence of the structure factor S . At larger system sizes, the nonequilibrium critical region will be even broader.

For the critical exponent η_ψ in the single-Dirac-fermion Hubbard model, a similar accuracy analysis is shown in Figs. R1e-f. The nonequilibrium scaling region for the fermion correlation G is much broader, and even with very small values of $(\tau L^{-z})_{\min}$, the results for η_ψ do not deviate significantly. With DSM initial state, as seen in Figs. R1e and f, we find that taking $(\tau L^{-z})_{\min} = 0.01$ is already sufficient for the convergence of η_ψ , with the data collapse also of high quality. The distribution of η_ψ obtained from resampling is shown in Fig. R1g, where a Gaussian fit gives $\eta_\psi = 0.134(3)$. The corresponding data collapse and scaling range are displayed in Fig. R1h. For the FM initial state, we take $(\tau L^{-z})_{\min} = 0.1$, which is sufficient for convergence, and obtain $\eta_\psi = 0.136(14)$.

The accuracy of the critical point is also self-consistently verified using the same method. For example, in the manuscript we take the DSM as the initial state and determine the critical point of the single-Dirac-fermion Hubbard model as $U_c = 7.220(37)$ at $\tau L^{-z} = 0.3$. In this revision, we have supplemented the data by extending τL^{-z} to 0.5, obtaining $U_c = 7.225(34)$, which is consistent with the result at $\tau L^{-z} = 0.3$ within the error bars [See Change 4(2)]. This demonstrates that our imaginary-time evolution has already entered the nonequilibrium scaling region and that the value of the critical point has converged. In addition, in the SM we also consider the FM initial state and obtain $U_c = 7.214(44)$ at $\tau L^{-z} = 0.5$, which is again consistent with the DSM initial-state result within the error bars. The agreement of the critical points obtained from different initial states further confirms the accuracy of our calculation.

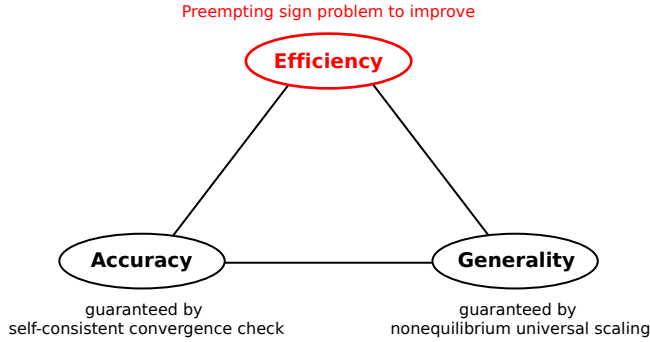


FIG. R2. Typically, without introducing additional physical priors, it is extremely challenging for an algorithm to simultaneously improve or maintain efficiency, accuracy, and generality [1]. However, our framework improves efficiency significantly by preempting the sign problem, while ensuring that accuracy and generality are not sacrificed through self-consistent convergence checks and the power of nonequilibrium universal scaling.

From the above analysis procedure, it is clear that determining critical points and critical exponents using nonequilibrium scaling is highly controllable in terms of accuracy. We can assess the accuracy not only by examining the asymptotic convergence and the quality of the data collapse, but more importantly, by the fact that nonequilibrium evolutions from different initial states are governed by the same ground-state critical exponents. **The consistency of the critical points and critical exponents obtained with different initial states is smoking gun evidence that our results are sufficiently accurate and self-consistent.** This is a significant advantage of the nonequilibrium approach compared with finite-temperature scaling or finite-size scaling in the conventional equilibrium approaches. Even in situations where the sign problem is particularly severe and prevents accurate results within the scaling range, the early-time results from different initial states can still bracket a controlled range for the critical points and critical exponent.

How does our method enhance computational efficiency without sacrificing accuracy and generality? We understand the reviewer's potential concern. Typically, without new physical input, improvements in algorithmic efficiency come at the cost of either generality or accuracy. For instance, some QMC algorithms can mitigate the impact of the sign problem to some extent but introduce biased results and uncontrolled systematic error. **We would like to emphasize that our framework is not simply an approximate computational technique that sacrifices accuracy and generality for efficiency gains.** Our method indeed incorporates more physical insights, including the scalable nonequilibrium data and multiple initial-state choices that can be controlled and self-consistently verified (Fig. R2). These pieces of information, traditionally discarded as divergent or invalid in PQMC methods, are precisely what we have recovered and utilized to reveal critical insights into the ground-state phase diagram and phase transition. This is the philosophical essence that makes our methodology effective.

Finally, We appreciate the reviewer's comment that “The data collapsing in Figs. 1e and 2c is not completely satisfactory.” This observation actually stemmed from a misleading presentation in our previous manuscript. Our data collapse analysis is *only* performed using data within the defined scaling range, which appears after a microscopic nonuniversal time scale. Data points at very small τL^{-z} lie outside this range and are, therefore, excluded from the analysis. As elaborated earlier in this response, the data points within the scaling range exhibit excellent data collapse, robustly obeying the scaling relation. This is quantitatively evidenced by the reduced chi-squared values of $\chi_{\nu}^2 = 1.241$ for Fig. 1e and $\chi_{\nu}^2 = 1.668$ for Fig. 2c. The χ_{ν}^2 values for the other data-collapse figures are also added in the manuscript [See Change 3(3)].

However, it should be emphasized that this is not the specific issue for the short-time scaling. Even for the more popular finite-size scaling, when the lattice size is too small to enter the scaling region, the finite-size scaling can lose its efficacy.

The boundary of this scaling range is critical for the practical application of our method, as it dictates the minimum permissible τL^{-z} and thus the extent to which the sign problem can be alleviated. For this reason, we deliberately presented the crossover from scaling violation to scaling satisfaction in these figures. This approach provides a direct visualization of the scaling-range boundary, elucidating our rationale for selecting appropriate τL^{-z} values and preventing the misconception that τL^{-z} can be chosen arbitrarily small. In the revised manuscript, we have now

explicitly marked the scaling range in these figures [See Changes 3(3), 4(4)] and included a detailed explanation of the technical procedures employed to accurately determine the critical exponents [See Changes 2(6), 2(7), 2(10), 4(2)]. We sincerely thank the reviewer for highlighting this point, which has significantly improved the clarity and quality of our manuscript.

Comment:

As I mentioned in my previous report, is it possible to distinguish between first- and second-order transitions during this very short-term evolution?

Reply:

We thank the reviewer for raising this important point. Although we did not find this specific comment explicitly mentioned in the previous report, we agree that it is a crucial issue to clarify [See Change 4(1)].

The scaling form in our theoretical framework relies on quantum criticality. In this framework, we can determine whether a continuous phase transition exists. The key criteria are: 1) For a given τL^{-z} , the crossing points of the correlation-length ratio or Binder ratio curves converge to a single point as the system size increases (dimensionless quantities exhibit scale invariance at the critical point). 2) The nonequilibrium critical relaxation processes of physical quantities such as the structure factor and fermion correlation display scaling collapse.

In fact, we are also able to identify a first-order phase transition during the short-time evolution through opposite characteristics: 1) The crossing points of the correlation-length ratio or Binder ratio curves do not converge to a single point. 2) The nonequilibrium critical relaxation processes of physical quantities such as the structure factor and fermion correlation cannot be well scaled to collapse. Additionally, 3) Due to the coexistence of two phases at a first-order phase transition, the Binder ratio typically shows negative dips at the transition point, and the Monte Carlo sampling distribution of the structure factor exhibits a double peak. The emergence of negative dips in the results of Binder ratio is a hallmark of the first-order transition.

As a typical example, we demonstrate how to identify the first-order phase transition in the $q = 6$ quantum Potts chain during short imaginary time evolution [See Change 4(1)]. The Hamiltonian is given by:

$$H = -qJ \sum_i \sum_{m=0}^{q-1} P_i^{(m)} P_{i+1}^{(m)} - h \sum_i \sum_{m \neq n} |m\rangle_i \langle n|, \quad (\text{R2})$$

where $P_i^{(m)} \equiv |m\rangle_i \langle m|$ is the projection operator on site i , and the tuning parameter is $g \equiv h/J$. For $g < 1$, the ground state is in the ferromagnetic phase, and for $g > 1$, it is in the paramagnetic phase. For the case of $q = 6$, a first-order phase transition occurs at $g_c = 1$. We use the time-evolving block decimation (TEBD) method to simulate

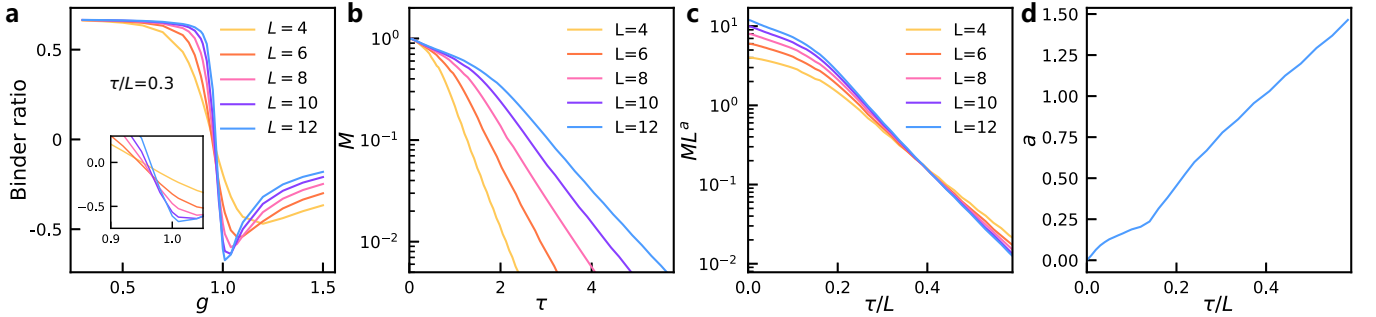


FIG. R3. **First-order phase transition characteristics in the $q = 6$ quantum Potts chain observed during short imaginary time evolution.** **a**, Binder ratio versus g for different system sizes, where the curves do not intersect at a single point, and negative dips are observed. The emergence of negative dips in the Binder ratios is a hallmark of first-order transition. **b**, Imaginary time relaxation of the order parameter M starting from the ordered phase at $g = 1$. **c**, Failure of scaling collapse for **b**, with $a = 1.0$ as an example. **d**, Fitting $M \propto L^{-a}$ for fixed τ/L , where the value of a does not converge as τ/L increases.

the system's imaginary time evolution starting from an ordered ferromagnetic initial state (e.g., all sites choosed into $m = 0$ state) and observe the order parameter M and Binder ratio R :

$$M \equiv \frac{1}{L} \sum_{i=1}^L s_i, \quad R \equiv 1 - \frac{\langle M^4 \rangle}{3 \langle M^2 \rangle^2}, \quad (\text{R3})$$

where $s_i \equiv \frac{q}{q-1} \left(P_i^{(0)} - \frac{1}{q} \right)$. Using the same procedure as in the manuscript, we take a short imaginary time $\tau/L = 0.3$. The variation of Binder ratio R with g is shown in Fig. R3a. The curves for different system sizes do not intersect at a single point, and there are distinct negative dips, which are characteristic of a first-order phase transition and can appear with short imaginary time evolution at $\tau/L = 0.3$. Fig. R3b shows the imaginary time relaxation of the order parameter M starting from the ordered phase at $g = 1$, which decays exponentially with τ . Fig. R3c demonstrates the failure of scaling collapse for M , using a scaling exponent $a = 1.0$ as an example. Adjusting a does not allow these curves to collapse or partially collapse. If we fix τ/L and perform scaling fitting according to the form $M \propto L^{-a}$, the results for a are shown in Fig. R3d, and they do not converge as τ/L increases. These results, which violate scaling forms, clearly exclude the possibility of a continuous phase transition here. This example illustrates that a first-order phase transition can be distinguished from a continuous phase transition even during short imaginary time evolution, and we have added this statement in the revised manuscript [See Change 2(9)].

Comment:

In addition to the initial benchmarks, the calculations for the SU(3) Hubbard model in presence of a staggered magnetic field are reported. Even though the authors offer some rationale for investigating this Hamiltonian, it is not a standard example within the field of strongly correlated systems. This is another reason I believe the paper lacks broad interest for a general audience. The authors suggest that the transition between the semi-metal and the antiferromagnetic insulator is not compatible with the Gross-Neveu universality class: again, this is a result that may be relevant for a very restricted community and not a general audience. At this stage, these results will not have a large impact on the community.

Reply:

We thank the reviewer for the important comments and feedback. While we acknowledge that the SU(2) Hubbard model is often considered more prototypical, our study of the SU(3) Hubbard model presents breakthroughs that specifically address less explored regimes and carry significant general interest and impact across strongly correlated systems, statistical physics, cold-atom experiments, and high-energy physics. (1) For strongly correlated models, the SU(N) Hubbard model is one of the most fundamental and standard examples, and we have, for the first time, revealed the ground-state phase diagram of the half-filled repulsive Hubbard model with odd N . (2) For the statistical physics community, we significantly extend the celebrated Gross-Neveu universality family beyond the classical O(N) ordering structures, which is also a topic of interest for the high-energy physics community. (3) For cold-atom physics experiments, SU(N) Hubbard physics has been a hot direction in recent years, and the SU(3) Hubbard model can already be realized in ultracold-atom optical lattices, where unbiased theoretical calculations are now urgently needed. (4) For high-energy physics, the SU(3) Hubbard model and the extended Gross-Neveu universality class can also have profound impacts. The successful application of our nonequilibrium short-time framework to the SU(3) Hubbard model has opened a new direction for studying quantum many-body systems and controlling the sign problem, with the potential to continue making breakthroughs on long-standing challenges across strongly correlated and statistical physics, quantum chemistry, and high-energy physics in the future.

Below we provide a detailed clarification of the general interest of the SU(3) Hubbard model across different fields.

1. For strongly correlated theories: SU(N) Hubbard model as one of the standard starting points

The Hubbard model is one of the most fundamental and influential theoretical models in condensed matter physics. When the flavor symmetry is generalized from SU(2) to SU(N), a host of novel quantum phases emerges, driven by enhanced quantum spin fluctuations as N increases. These include intriguing phenomena such as spin liquids [2–7], color superfluids [8, 9], trionic bound states/composite fermions [9–12], exotic pairing and dynamical scar states [13–17]. Therefore, SU(N) strongly correlated fermionic systems beyond SU(2) symmetry have been a long-standing focus of the community, serving as a fertile ground to explore the rich and

exotic phenomena arising from various ingredients in quantum many-body systems. Moreover, these systems are not just theoretical playground; they are realized in the cutting-edge two-dimensional materials such as twisted bilayer graphene, which inherently incorporates multi-degrees of freedom including valley, spin, and layers [18–23]. Extensive studies have already covered a wide range of strongly correlated models, with diverse theoretical methods applied in persistent efforts to understand the underlying physics [5, 7, 9, 24–39]. **Among them, the $SU(N)$ Hubbard model is the most fundamental and prototypical example, attracting the broadest interest, with various values of N and lattice geometries widely discussed** [2, 6, 8, 12, 15–17, 25–27, 30–32, 34, 36, 39–72].

Strongly interacting Dirac systems is a very active research field in modern condensed matter physics, since they not only incarnate the relativistic fermions with linear dispersion in high-energy physics into the field of condensed matter physics, but also have significant potential application value, as indicated by groundbreaking discoveries of graphene [73] and topological insulators [74, 75]. In these systems, a rapidly growing direction is the $SU(N)$ Hubbard model with Dirac fermions, where strong correlation effects are hypothesized to not only induce a gap but also drive exotic phases and quantum phase transitions. This also deeply connects to high-energy physics and statistics physics, where the spontaneous symmetry breaking of $SU(N)$ Dirac fermions—governed by the Gross-Neveu-Yukawa theory—is a key aspect of quantum phase transitions [76, 77]. Moreover, a particularly exciting development is the proposal that $SU(N)$ Dirac fermions serve as the effective description for two-dimensional moiré materials, such as twisted bilayer graphene [22, 23]. This provides a unique and powerful experimental platform to directly probe strong correlation phenomena and quantum criticality in $SU(N)$ Dirac systems.

However, even for the most typical $SU(N)$ Dirac fermion models with usual repulsive Hubbard interaction, an awkward situation appears in which colorful phase and phase transitions have been theoretically explored for even N cases, such as the basic $SU(2)$ Hubbard model [78, 79], $SU(4)$ cases [6, 47, 68], and $SU(6)$ cases [47], **but the quantum phases and their transitions with odd N are still largely in a state of research blank** [80].

This apparently does not imply that the repulsive Hubbard model for odd N is unimportant. In fact, there are many clues pointing to new physics in these system, potentially more non-trivial than for even N . For instance, in the strong interaction limit, the half-filled Hubbard model with even N can be mapped to a spin Heisenberg model, but for the odd N case, where the average particle number is half-integer (similar to a frustration effect), there is no perfect spin model counterpart. The intrinsic charge fluctuations of the fermions remain significant even in the strong interaction limit [36]. The $SU(N)$ Hubbard model with odd N differs fundamentally from the even N case, especially for smaller N [36]. Thus, can the $SU(N)$ Dirac fermions with odd N acquire mass through Hubbard interactions? Do charge fluctuations prevent the formation of spin magnetic order? What is the phase diagram of the model? Can the phase transition be described by the Gross-Neveu-Yukawa theory, and if so, how? All these questions are waiting for us to explore.

However, a sharp contradiction between the intense desire to explore novel states of matter in these systems and the scarcity of effective computational tools has appears in this field. **The enormous barrier standing between the problem and the answer is the notorious sign problem.**

For the sign-problematic $SU(N)$ Hubbard models with odd N , our work has taken a step forward by performing the first unbiased numerical calculation. We consider a minimal strongly interacting model featuring Dirac fermions beyond $SU(2)$, namely the staggered-flux $SU(3)$ Hubbard model. We are the first to solve the ground-state phase diagram of this model and determine the critical exponents and universality class of the phase transition, which differ significantly from the case of even N .

We believe this is an important starting point in the field of strongly correlated systems, and our method is also promising for solving other sign-problematic $SU(N)$ strongly correlated models, or the doped Hubbard model with general Fermi surface. As a very typical and standard example of strongly correlated models, our breakthrough is crucial for the entire strongly correlated community.

2. For statistical physics: fundamentally reshaping current understanding of Gross-Neveu criticality

Universality class is the core organizing principle in the theory of phase transitions. Continuous phase transitions, even occurring in quite distinct systems, can exhibit similar scaling behaviors described by the same set of critical exponents, as long as they belong to the same universality class. Accordingly, the numerous and complex phase transitions in nature can be classified into a relatively small number of universality classes. The discovery of new universality class can undoubtedly advance our understanding of statistical physics.

The Gross-Neveu universality classes, describing phase transitions where massless Dirac fermions acquire a mass accompanied by spontaneous symmetry breaking that generates bosonic order parameters, represents the most

typical phase transitions in Dirac systems. (1) *Historically*, the most prominent example of the Gross-Neveu universality classes have long been regarded as the chiral $O(N)$ universality class. As a direct generalization of the $O(N)$ universality class, the chiral $O(N)$ universality class contributes fertile fermionic critical properties, which are not only beyond the quantum-classical mapping but also beyond the Landau's paradigm in some cases, attracting extensive investigations in last two decades. (2) *Presently*, our work uncovers an unconventional Gross-Neveu transition that belongs to a new chiral $SU(3)$ universality class, which significantly extends the scope of the Gross-Neveu universality classes.

In the following, we provide a comparative introduction to the traditional chiral $O(N)$ universality class and the new chiral $SU(3)$ universality class. To avoid confusion, we here use N to denote the dimension of the classical order parameter, N_b to denote the dimension of the bosonic order parameter, and N_f to denote the number of fermion flavors.

Traditional chiral $O(N_b)$ universality class— In three-dimensional classical systems or 2+1 dimensional quantum systems, the most typical $O(N)$ universality classes widely describe a variety of important phase transitions, such as the gas-liquid transition of simple gases, the superfluid transition of liquid helium, and the Heisenberg transition of ferromagnets. Specifically, the $N = 1$ case is referred to as the Ising universality class, $N = 2$ as the XY universality class, and $N = 3$ as the Heisenberg universality class. Their critical behaviors can be simply described by purely bosonic ϕ^4 theories with $O(N)$ symmetries.

When the boson order parameter fields are coupled to Dirac fermions, the critical properties are significantly modified by the gapless fermion fluctuations, which leads to the definition of the “chiral versions” of the above universality classes [77], namely the *chiral $O(N_b)$* universality classes. For example, quantum phase transitions with a Z_2 charge-density-wave order parameter belong to the *chiral Ising* universality class; those with an $O(2)$, or equivalently $U(1)$, superconducting order parameter belong to the *chiral XY* universality class; and those with an $O(3)$ antiferromagnetic order parameter belong to the *chiral Heisenberg* universality class. The corresponding low-energy effective field theories at criticality are obtained by coupling the ϕ^4 bosonic theory of the order parameter to chiral fermion fields through Yukawa terms, and can generally be written as

$$\mathcal{L} = \text{tr}(\bar{\psi}\partial^\mu\psi) + g \text{tr}(\bar{\psi}\Phi\psi) + \text{tr}((\partial_\mu\Phi)^2) + r \text{tr}(\Phi^2) + \lambda (\text{tr}(\Phi^2))^2, \quad (\text{R4})$$

where ψ is the fermion spinor field, and tr denotes the trace over the N_f flavors of chiral fermions with $SU(N_f)$ symmetry. The operator $\Phi = \sum_{i=1}^{N_b} \phi_i L_i$ spans an N_b -dimensional linear representation of the $SU(N_f)$ algebra, with N_b linearly independent bosonic components, and the N_f -dimensional matrices L_i form an orthogonal basis of this representation, such that $\text{tr}(\Phi^2) = \sum_{i=1}^{N_b} \phi_i^2$. This theory is the well-known Gross-Neveu-Yukawa theory. Therefore, these chiral $O(N_b)$ universality classes are collectively referred to as the *Gross-Neveu universality classes*. Their order parameters correspond to the N_b -dimensional real linear representation of the fermionic $SU(2)$ algebra, which happens to carry a faithful representation of the $O(N_b)$ group. Consequently, the bosonic fields in the theory also possess $O(N_b)$ symmetry, establishing a one-to-one correspondence with the usual $O(N)$ universality classes. We summarize in Table R1 the theoretical symmetries and the vacuum manifolds (ground-state degeneracy manifolds) after spontaneous symmetry breaking corresponding to various chiral $O(N_b)$ universality classes.

Due to the typicality and importance of the chiral $O(N_b)$ universality classes, the critical properties therein have been studied in a variety of lattice models with the aid of state-of-the-art numerical methods [78, 79, 81–87]. In addition, controllable results have also been obtained through various analytical approaches [88–93]. These results show good consistency, providing strong support for the effectiveness of the Gross-Neveu-Yukawa theory (R4) in describing Dirac criticality.

New Chiral $SU(3)$ universality class— A fundamental question of broad interest across statistical physics, condensed matter physics, and high-energy physics is whether fermionic Gross-Neveu criticality can arise that goes beyond the $O(N)$ counterparts.

In this work, we find that $SU(N_f)$ Dirac fermion systems with odd N_f offer precisely such a pathway. From the perspective of the structure of symmetry group algebras, the key distinction between odd and even N_f lies in the fact that $SU(N_f)$ groups with odd N_f cannot be isomorphic to spin groups, which may allow for the emergence of “more fermionic” universality classes, as illustrated in Fig R4. For even N_f , however, at small values of N_f , such as $SU(2)$ and $SU(4)$, the groups are locally isomorphic to $O(3)$ and $O(6)$, respectively; while at large N_f , the system typically does not favor breaking $SU(N_f)$ symmetry to form spin order, but instead tends to form a valence-bond solid [94, 95]. Indeed, all Gross-Neveu transitions studied so far for even N_f fall

TABLE R1. Comparison of the symmetries of different Gross-Neveu universality classes. The symmetries of the theories and the vacuum manifolds (ground-state degeneracy manifolds) after spontaneous symmetry breaking are listed. Each chiral $O(N_b)$ universality class corresponds to an $O(N)$ universality class with the same symmetries and vacuum manifold. In contrast, the new chiral $SU(3)$ universality class reported in our manuscript has no corresponding $O(N)$ universality class.

Gross-Neveu classes	Symmetry	Vacuum manifold
chiral $O(N_b)$	chiral Ising	S^0
	chiral XY	S^1
	chiral Heisenberg	S^2
chiral $SU(3)$	$SU(3) \times Z_2$	$\frac{SU(3) \times Z_2}{SU(2) \times U(1)} (\simeq \mathbb{CP}^2 \times Z_2)$

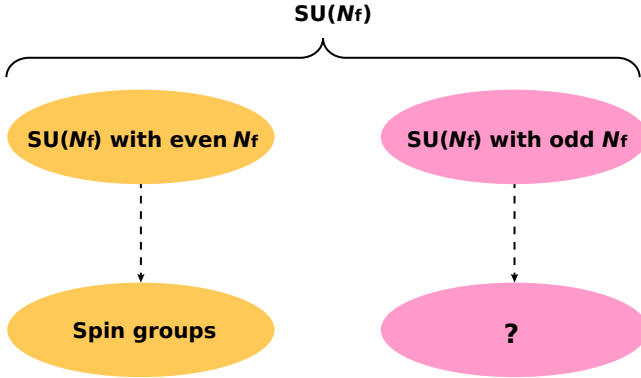


FIG. R4. For odd N_f , the $SU(N_f)$ group cannot be isomorphic to a spin group, which may give rise to new Gross-Neveu universality classes that more directly manifest the spinor nature of fermions.

back into the conventional chiral $O(N_b)$ universality classes [6, 34, 52, 96–98]. Therefore, investigating the case of odd N_f is of fundamental importance for understanding fermionic phase transitions.

We clearly identify the first nontrivial fermionic Gross-Neveu criticality that goes beyond the $O(N)$ order-parameter structures. The continuous transition from the $SU(3)$ DSM to the λ_8 -AFM phase reported in our manuscript belongs to the Gross-Neveu universality class family but does not fall into any of the known chiral Ising, chiral XY, or chiral Heisenberg classes. In the λ_8 -AFM phase, the order parameter spontaneously selects the λ_8 direction of the $SU(3)$ algebra. Under $SU(3)$ transformations, this order parameter transforms according to the 8-dimensional adjoint representation of $SU(3)$ and spans a 4-dimensional $\frac{SU(3) \times Z_2}{SU(2) \times U(1)}$ manifold, which is nonlinearly embedded in \mathbb{R}^8 . $SU(3)$ cannot be isomorphic or locally isomorphic to any other classical linear groups, which is in sharp contrast to the cases of even N_f such as $SU(2)$ and $SU(4)$. Therefore, the new $SU(3)$ antiferromagnetic order parameter we have discovered does not have a corresponding $O(N_b)$ order parameter. In addition to the symmetry analysis, our QMC results unbiasedly determine the critical exponents of this new universality class. As shown in Table S4 of the Supplementary Materials, its critical exponents differ from those of the chiral Ising, chiral XY, and chiral Heisenberg universality classes, which provides compelling evidence that this new universality class cannot be categorized into the existing chiral $O(N_b)$ Gross-Neveu universality classes. We temporarily refer to this new universality class as the *chiral $SU(3)$* universality class. Table R1 summarizes the differences of this new universality class from the previously known ones in terms of symmetry and vacuum manifold.

The nontrivial new Gross-Neveu universality class we discovered represents the first minimal example of a Gross-Neveu transition without a classical $O(N)$ correspondence. As illustrated in Fig. R5, our results demonstrate that the Gross-Neveu universality class encompasses a broader and nontrivial set with intrinsic fermionic characteristics. This significantly broadens the theory of quantum phase transitions and opens up a new and rich research field in statistical physics. The most direct new question is: what kind of Gross-Neveu-Yukawa theory should be used to describe the low-energy effective field theory of this transition? Since the bosonic field does not possess $O(N_b)$ symmetry, its form is likely different from the previous expression in Eq. (R4). We conjecture

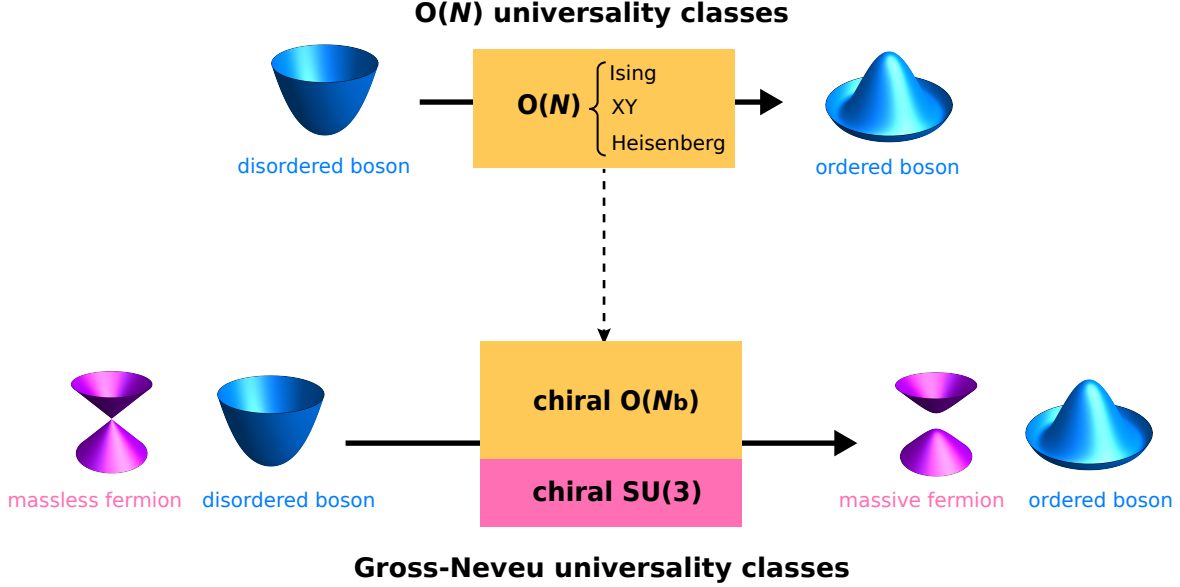


FIG. R5. Schematic illustration of the relationship between $O(N)$ universality classes and Gross-Neveu universality classes. The $O(N)$ universality classes, including Ising, XY, and Heisenberg, describe spontaneous symmetry breaking with an $O(N)$ order parameter. The Gross-Neveu universality classes describe the situation where, along with spontaneous symmetry breaking of the bosonic order parameter, massless Dirac fermions also spontaneously acquire a mass. Within the Gross-Neveu universality classes, the traditional chiral $O(N_b)$ universality classes correspond one-to-one to the $O(N)$ universality classes, whereas the chiral $SU(3)$ universality class in the Gross-Neveu universality classes does not possess an $O(N_b)$ order-parameter structure and instead represents a fermion-intrinsic universality class.

that it may take the following form:

$$\mathcal{L} = \text{tr}(\bar{\psi}\not{\partial}\psi) + g \text{tr}(\bar{\psi}\Phi\psi) + \text{tr}[(\partial_\mu\Phi)^2] + r \text{tr}(\Phi^2) + \lambda [\text{tr}(\Phi^2)]^2 + a [\text{tr}(\Phi^3)]^2 + c [\text{tr}(\Phi^2)]^4, \quad (\text{R5})$$

where $\Phi = \sum_{i=1}^{N_b} \phi_i \frac{\lambda_i}{2}$, $N_b = 8$ spans the 8-dimensional adjoint representation of $SU(3)$. Compared with Eq. (R4), the marginal term $a [\text{tr}(\Phi^3)]^2$ is introduced to reduce the $SO(8)$ symmetry of the bosonic field to $SU(3) \times Z_2$ symmetry, while the irrelevant term $c [\text{tr}(\Phi^2)]^4$ with $c > 0$ is also introduced to ensure vacuum stability. Due to the $SU(3)$ algebra identity $\text{tr}(\Phi^3) = 3 \det \Phi$, only the ϕ_8 component of the order parameter along the λ_8 direction with full rank contributes a nonzero value to $[\text{tr}(\Phi^3)]^2$. Therefore, when $a < 0$, the $SU(3)$ -symmetric bosonic field tends to spontaneously break toward the λ_8 direction. This is very different from the $O(N)$ or $O(N_b)$ symmetry breaking triggered by $r < 0$ in the ϕ^4 theory. Whether such a Gross-Neveu-Yukawa theory can capture the new universality class we discovered (for example, yielding critical exponents consistent with our numerical results) remains an open question for future study. At the same time, such an order parameter that carries an $SU(3)$ bilinear representation rather than an $O(N_b)$ linear representation may also be constructed through a recent theoretical framework with tensorial criticality [99–101], which is also worth exploring. Moreover, beyond the first nontrivial chiral $SU(3)$ universality class that we have found, can more nontrivial Gross-Neveu transitions be realized in lattice models? We believe these questions will attract very broad interest.

We sincerely thank the reviewer for drawing our attention to the wording issue in the original manuscript. The reviewer considered this transition not to belong to the Gross-Neveu universality classes, which was regarded as an important reason why the manuscript might not appeal to a general audience. This indicates that our earlier phrasing caused a serious misunderstanding. In the revised version, we have corrected this issue and explicitly stated that we believe the new transition we discovered belongs to a new nontrivial Gross-Neveu universality class [See Changes 1, 2(3), 2(9), 2(11), 4(3)]. It represents the first minimal example of a Gross-Neveu transition without a classical $O(N)$ order structure, which significantly broadens the Gross-Neveu universality

classes. Therefore, taking the reviewer's comments into account, we believe that our manuscript will attract wide interest from a general audience. We hope that our revisions can eliminate the previous misguidance.

3. For cold-atom experiments: the $SU(N)$ Hubbard model is currently generating a wave of research interest

The quantum simulation of the $SU(N)$ Hubbard model has become one of the mainstream research directions in the field of cold-atom physics, and it has grown increasingly active in recent years. Alkaline-earth atoms such as ^{87}Sr and alkaline-earth-like atoms such as ^{173}Yb , owing to their nuclear spins exhibiting $SU(2I+1)$ -symmetric repulsive interactions, can be loaded into optical lattices to realize the $SU(N)$ Hubbard model. Under magnetic-field control, the value of N can currently be tuned from 2 up to 10 [24]. After more than a decade of development, this technique has become highly mature [24, 102–107]. Moreover, with the advancement and application of quantum gas microscopy [108–110], number-resolved imaging [111], and cooling techniques specifically designed for $SU(N)$ gases [112, 113], experiments are now capable of measuring long-range correlations and exploring various magnetic states. At present, investigating the Mott transition and magnetic ordering in the $SU(N)$ Hubbard model is a hot topic of joint interest in both cold-atom experiments and strongly correlated physics theories.

The $SU(3)$ Hubbard model has already been realized in ultracold alkaline-earth atomic systems in optical lattices. For example, in recent years the Munich group has studied the $SU(3)$ Hubbard model in both 3D and 2D optical lattices, observed experimental signatures of the Mott crossover, and achieved high-precision characterization of the equation of state (density-chemical potential relation) [103, 107]. By fitting the experimental equation-of-state data with numerical methods such as DQMC, they obtained temperature calibration for the experimental system with excellent agreement [107]. This suggests that the novel quantum criticality and magnetic order we have uncovered through unbiased PQMC calculations in the $SU(3)$ Hubbard model are very promising to be realized in such experimental systems. In a recent experiment, the Florence group realized flavor-selective Mott localization in an $SU(3)$ Fermi gas in a 3D optical lattice [106]. Under conditions that break $SU(3)$ symmetry, they observed an ordered state quite similar to our λ_8 -AFM. Such systems thus offer immense potential for realizing the novel Gross-Neveu Dirac quantum criticality we predict.

On the other hand, some experimental progress has already gone beyond the range accessible to previous theoretical calculations. For example, high-precision measurements of antiferromagnetic correlations in the $SU(2)$, $SU(4)$, and $SU(6)$ Hubbard models have been reported [104, 105]. Their results are consistent with numerical calculations from parameter-free DQMC in the high-entropy (high-temperature) regime, but in the low-entropy (low-temperature) regime in three dimensions, deviations from the DQMC results remain. Moreover, some of the experimental data have reached extremely low entropy values, exceeding the regime where numerical simulations converge [105]. In fact, at the temperatures relevant to the experiments, there exists a severe sign problem, and DQMC sampling already suffers from non-ergodicity, making it difficult to obtain controlled results [59]. The rapid progress in cold-atom experiments is clearly calling for the development of more advanced numerical techniques to alleviate the sign problem [24, 105]. Our new method of preempting the sign problem to solve the zero-temperature ground-state phase diagram shows great potential for interpreting these experimental results.

In summary, not only will the $SU(3)$ Hubbard ground-state phase diagram and the novel Gross-Neveu transition presented in our manuscript provide clear theoretical guidance for the rapidly developing field of cold-atom experiments, but also the advanced method we propose for alleviating the sign problem is crucial for understanding experimental results that lie beyond the reach of existing computational approaches.

4. For high-energy physics: the $SU(3)$ Hubbard model and the Gross-Neveu universality class also attract attention

$SU(3)$ -symmetric strongly coupled systems have drawn even greater attention in the field of high-energy physics. The Gross-Neveu theory was originally introduced by the high-energy physics community as a toy model for quantum chromodynamics (QCD), since it captures important phenomena such as asymptotic freedom, chiral symmetry breaking, and dynamical mass generation [76]. As the simplest platform for nonperturbative fermionic CFTs, the critical exponents of the Gross-Neveu universality class have been computed by the high-energy community using methods such as the ϵ -expansion near the critical dimension, large- N expansion, Monte-Carlo simulation and conformal bootstrap [77, 88–93, 114]. Historically, these studies have predominantly focused on chiral Ising, chiral XY, and chiral Heisenberg universality classes, limited by existing theoretical approaches and

knowledge of this universality family. Our discovery of the Gross-Neveu universality class with SU(3) order-parameter structure broadens the understanding in high-energy physics and will certainly attract a series of further in-depth investigations.

In addition, the half-filled SU(N) Fermi-Hubbard model has recently been constructed within the AdS/CFT framework at the supergravity limit of D-branes [115], where N corresponds to the ultraviolet input parameter at the open-string boundary [116] and its odd-even parity affects the massless spectrum of open strings [115]. Our manuscript provides unbiased quantitative results for the Hubbard model with odd N , offering a rare numerical benchmark for testing the applicability of the AdS/CFT conjecture in strongly correlated systems.

To conclude, our work on the SU(3) Hubbard model holds significant and broad impact, bridging diverse fields such as strongly correlated physics, statistical physics, cold atoms, and high-energy physics. This wide-ranging relevance ensures it is not confined to a narrow specialization.

The successful application of our nonequilibrium short-time framework to the SU(3) Hubbard model is an exciting starting point. This framework opens up a new direction for studying quantum many-body physics, particularly in confronting the notorious ‘sign problem’—a bottleneck for progress in strongly correlated physics, statistical physics, quantum chemistry, and high-energy physics. Moving forward, this approach holds the potential to resolve long-standing debates within these fields by enabling large-scale, unbiased numerical simulations. Below we elaborate with relevant contexts and examples:

1. Potential applications in strongly correlated and statistical physics

Our team has in fact already started to apply this framework to other long-standing challenging problems in strongly correlated physics and has obtained some preliminary results. Below, we present some unpublished early results to further demonstrate the power of the nonequilibrium framework.

The first example is about the interaction driven topological phase of quantum anomalous Hall (QAH) effect. The Chern insulator featuring quantum anomalous Hall (QAH) effect is a corner stone in the research of condensed matter physics. A central challenge for researchers is to understand how a Chern insulator can spontaneously arise from electronic interactions within a basic microscopic model. In 2008, S. Raghu and collaborators introduced an extremely simple interacting model, the half-filled spinless fermion model on a honeycomb lattice featuring next-nearest-neighbor repulsive interaction [117]:

$$H = -t \sum_{\langle ij \rangle} c_i^\dagger c_j + V \sum_{\langle\langle ij \rangle\rangle} n_i n_j \quad (\text{R6})$$

The model is governed by a single parameter V/t . When $V = 0$, the ground state of the model is a Dirac semimetal (DSM). S. Raghu et al. pointed out through mean-field analysis the emergence of a Chern insulator exhibiting QAH effect may when V is large [117]. However, the ground-state phase diagram of this model, and specifically the existence of the QAH regime, has remained unsettled to this day [118–126]. A comparison of phase diagrams obtained from different works is shown in Fig. R6. Early mean-field analyses all indicated that as V increases, there exists a DSM-to-QAH phase transition [117–119]. Later exact diagonalization (ED) studies [120–122] on small-size systems showed that for larger values of V , it is more likely for a charge modulation (CM) phase to appear, namely a charge density wave with momentum at the Dirac points $K = (\pm \frac{4\pi}{3}, 0)$. Among these ED works, the largest lattice size used was in Ref. [122], which computed up to $N = 42$ sites. A similar phase diagram was also obtained with density matrix renormalization group (DMRG) calculations on a semi-infinite cylinder of width $L_y = 12$, keeping up to 1600 states [123]. The functional renormalization group (FRG) technique yielded a phase diagram suggesting that the QAH phase might appear at even larger values of V [124].

Due to the presence of severe sign problem, previous QMC methods were unable to solve this model. As an application of the nonequilibrium short-time QMC framework introduced in this manuscript, we currently take a shorter imaginary time $\tau = 0.25L$ and choose the initial state as the CM state to obtain a milder sign problem. We define the QAH structure factor S_{QAH} and correlation length ratio R_{QAH} as:

$$S_{\text{QAH}}(\mathbf{k}) = \frac{1}{L^4} \sum_{ij\alpha\Delta} e^{i\mathbf{k}\cdot(\mathbf{r}_i - \mathbf{r}_j)} \left\langle J_i^{(\alpha, \Delta)} J_j^{(\alpha, \Delta)} \right\rangle, \quad R_{\text{QAH}} = 1 - \frac{S_{\text{QAH}}(\mathbf{k} = \delta\mathbf{k})}{S_{\text{QAH}}(\mathbf{k} = \mathbf{0})}, \quad (\text{R7})$$

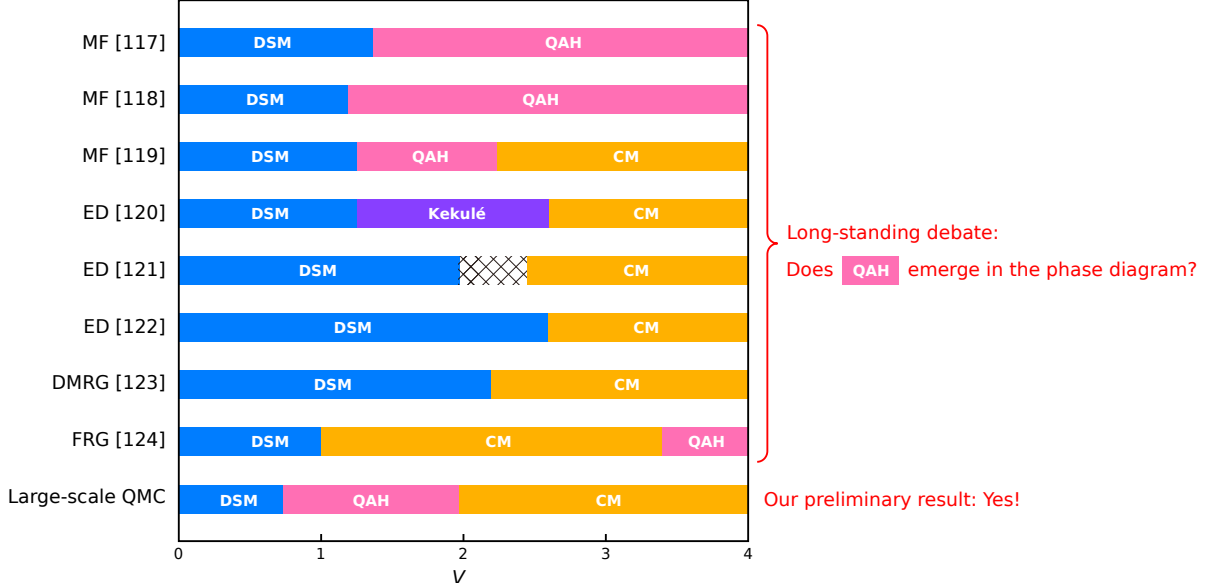


FIG. R6. Comparison of phase diagrams for the next-nearest-neighbor spinless t - V model obtained by different methods. [117–119] used the mean-field approximation. [120–122] employed the exact diagonalization method, among which [122] reached up to $N = 42$ sites. [123] used the density matrix renormalization group method on a semi-infinite cylinder of width $L_y = 12$, keeping up to 1600 states. The results in [124] were obtained using the functional renormalization group method. Our preliminary results are based on the nonequilibrium PQMC framework proposed in this manuscript (see Fig. R7 for details).

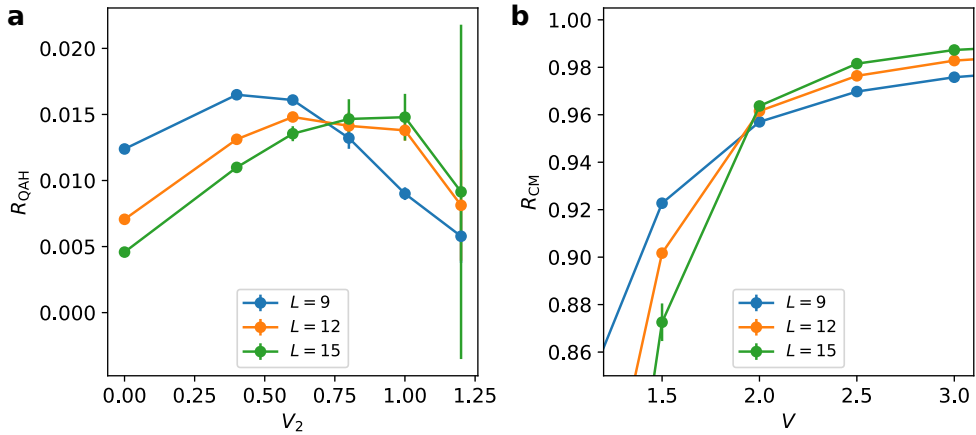


FIG. R7. Probing the phase diagram using the nonequilibrium short-time PQMC method. The initial state is chosen as the CM state, and the imaginary time is taken as $\tau = 0.25L$. **a**, Variation of the QAH current-current correlation length ratio R_{QAH} with V for different system sizes L . In the region $V = 0.3 \sim 0.5$, R_{QAH} increases with increasing L , which is a characteristic of the QAH phase. **b**, Variation of the CM correlation length ratio R_{CM} with V for different system sizes L . In the region where $V > 2$, R_{CM} increases with increasing L , which is a characteristic of the CM phase.

where the next-nearest-neighbor current operator $J_i^{(\alpha,\Delta)} = i(c_{i,\alpha}^\dagger c_{i+\Delta,\alpha} - c_{i+\Delta,\alpha}^\dagger c_{i,\alpha})$, $\alpha = 1, 2$ denotes the sublattices of the honeycomb lattice and $\Delta = 1, \dots, 6$ denotes different next-nearest-neighbor directions. We define the CM structure factor S_{CM} and the correlation length ratio R_{CM} as:

$$S_{CM}(\mathbf{k}) = \frac{1}{L^4} \sum_{ij\alpha} e^{i\mathbf{k}\cdot(\mathbf{r}_i-\mathbf{r}_j)} \left\langle \left(n_i^{(\alpha)} - \frac{1}{2} \right) \left(n_j^{(\alpha)} - \frac{1}{2} \right) \right\rangle, \quad R_{CM} = 1 - \frac{S_{CM}(\mathbf{k} = K + \delta\mathbf{k})}{S_{CM}(\mathbf{k} = K)}, \quad (\text{R8})$$

where $S_{CM}(\mathbf{k} = K)$ is the structure factor of the CDW with momentum K . The behavior of the correlation length ratio we obtained is shown in Fig. R7. The largest system size we have calculated so far reaches $L = 21$,

i.e., $N = 882$ sites, which is much larger than the maximum of 42 sites in previous ED calculations [122]. At present, in the intermediate region of V , namely $V = 0.3 \sim 0.5$, we observe that the QAH correlation length ratio R_{QAH} increases with increasing system size L , indicating a clear presence of a QAH phase in this region. In contrast, for $V > 2$, R_{CM} increases with increasing system size L , suggesting that at large values of V the system is in a CM phase.

These early results represent only a portion of our ongoing investigation. We will systematically test the self-consistent convergence of the phase transition point using various initial states and imaginary times. Crucially, our current results have already provided strong evidence for the existence of QAH in this model. At present, only our non-equilibrium short-time QMC framework can perform such large-scale unbiased calculations, capable of giving a definitive answer to the long-standing debate over the phase diagram.

Beyond the unbiased numerical results for the QAH in the spinless interacting Dirac-fermion model, we also apply our approach to a distinct class of fermionic QCPs: metallic QCPs, within a study nearing completion. Unlike Dirac QCPs, metallic QCPs feature a Fermi surface of gapless fermions. We investigate the ionic Hubbard model, where previous QMC studies were limited to high temperatures due to the sign problem [127, 128]. Those studies suggested a metallic phase emerging between CDW band insulator and AFM Mott insulating phases. By employing our short-imaginary-time relaxation approach, we are able to access the ground-state phase diagram and provide compelling evidence of this intermediate quantum metal phase. More crucially, for the first time, we characterize the quantum critical properties of the QCP between this quantum metal phase and the AFM ordered phase. These critical properties are distinct from the conventional 2+1d Heisenberg universality class, thereby further underscoring the versatility of our methodology.

Furthermore, our approach extends beyond calculating order parameter-related observables near QCPs. In another nearly-finished study, we utilize the short-imaginary-time scaling behaviors during relaxation to investigate entanglement entropy. Specifically, our short-imaginary-time framework enables us to extract the universal coefficient in the subleading corner correction of the entanglement entropy—a crucial universal parameter that encapsulates the fundamental characteristics of conformal field theory. This framework significantly enhances the computational efficiency for extracting entanglement information at QCPs, thereby further highlighting the profound and innovative impact of our research.

Given its profound capacity to resolve critical, long-standing problems in strongly correlated models, our proposed method unequivocally demonstrates its broad impact. It is indeed sufficient to open up a new field of numerical computation, and is definitely not “be relevant for a very restricted community.”

2. Potential applications in quantum chemistry

The ab initio solution of electronic structure problems has long been a focus in theoretical and computational chemistry. For transition-metal elements beyond the main group, strong correlation effects, also known as multi-reference character, render standard DFT methods invalid. For molecular systems with high degrees of freedom, the well-established coupled-cluster methods also face prohibitively high computational costs. To address these challenges, over the past two decades computational chemists have introduced a wide variety of QMC-based quantum chemistry algorithms [129–139]. Owing to their high accuracy and relatively low computational cost, these methods have already demonstrated great power in accurate calculations of diverse chemical systems, including small but challenging molecules, simple transition-metal complexes, solids, and organometallic compounds. However, the sign problem remains one of the most critical bottlenecks in quantum chemistry. Once the sign problem arises, current QMC methods for quantum chemistry either face exponential computational cost (e.g., full configuration interaction quantum Monte Carlo [130, 131], density matrix quantum Monte Carlo [133, 134]), or are forced to introduce subtle approximations (e.g., auxiliary-field quantum Monte Carlo based on trial-wavefunction approximations [132, 135, 136], diffusion Monte Carlo based on the fixed-node approximation [129, 138, 139]). In recent years, various attempts have been made in quantum chemistry to alleviate the sign problem [135, 138]. Our new framework of preempting the sign problem is relatively general and easy to use, and it holds great promise for integration with these QMC methods in quantum chemistry (requiring only minor modifications of the projection scheme). We believe our manuscript will therefore also attract broad interest from the quantum chemistry community.

3. Potential applications in high-energy physics

The QCD phase diagram, especially the possible QCD critical point (a.k.a. critical end point) that characterizes the transition between the hadronic phase and the quark-gluon plasma, is one of the holy-grail problems in QCD, and tremendous efforts have been devoted to it both experimentally and theoretically for decades [140]. Because

sign problems severely hinder unbiased lattice QCD simulations at finite density (finite chemical potential), the very existence and the location of the QCD critical point remain unsettled [140–144]. However, this problem is particularly well suited to be addressed by the Monte Carlo framework based on critical scaling theory that we propose in this manuscript. Scaling theory of the QCD critical point, including nonequilibrium criticality, has already received growing attention in the high-energy physics community [145–148]. Building on this foundation, our work will provide important insight to lattice QCD practitioners and may enable breakthroughs in numerically locating the QCD critical point, which would be highly valuable for understanding heavy-ion collider physics, the early universe, and neutron star structure.

In summary, the short-time scaling framework we propose for preempting the sign problem holds tremendous potential for future applications. Our ground-state solution of the SU(3) Hubbard model represents the first nontrivial step on this new path. Both the solution of the SU(3) Hubbard model and the control of the sign problem are important problems with broad interdisciplinary appeal and far-reaching impact. Encouraged by the reviewer's valuable suggestions, we have discussed the significance of our work and its future prospects in greater depth in the revised manuscript [See Changes 2(10), 2(11), 2(12)]. We sincerely thank the reviewer for the comments in this regard.

Comment:

In summary, I insist that the work is nice and may be published in more specialized journals, but not on *Science Advances*.

Reply:

We sincerely appreciate the reviewer's insightful comments, which have been instrumental in significantly enhancing the quality of this revised manuscript. In this revision, guided by the reviewer's helpful questions, we have conducted a more systematic analysis and incorporated substantial new numerical results, thereby thoroughly demonstrating the accuracy and reliability of our newly developed approach. We are deeply grateful for the valuable questions raised by the reviewer. Moreover, in the revised manuscript, we have endeavored to elucidate the broad appeal of our findings across diverse scientific domains, owing to the following two reasons:

We would like to emphasize once again that the SU(3) Hubbard model we study has general interest. As a paradigmatic strongly correlated model, it has attracted attention from both the strongly correlated theory community and the cold-atom experimental community. Its ground-state phase diagram has long been an interesting yet unresolved problem, until our work provided the answer. The new universality class of phase transitions we have discovered reshapes the understanding of the Gross-Neveu universality class in both the statistical physics and high-energy physics communities, and will undoubtedly trigger a new wave of research.

More crucially, our new framework opens up a novel direction for the study of quantum many-body physics. By enabling large-scale numerical simulations to overcome the shadow of the sign problem, it not only holds the promise of resolving many long-standing mysteries in condensed matter physics, but may also shed light on the QCD phase diagram in high-energy physics and on multireference problems in quantum chemistry.

We believe that these thorough discussions and revisions are sufficient for the reviewer to reassess the impact of this manuscript, for which we would be most grateful.

Far from being a narrow technical hurdle, the sign problem stands as a foundational and pervasive challenge impacting a vast spectrum of scientific communities. Both *Science* and *Science Advances* have published several articles purely focused on the sign problem [128, 149–151]. Indeed, as precisely noted by Reviewer 1, our paper is “an interesting paper proposing a new way around a major bottleneck in an important field”. Given this significant progress on such a critical and widespread problem, our work strongly merits publication in *Science Advances* due to its paramount importance, innovative contribution, and extensive general appeal.

[1] D.H. Wolpert and W.G. Macready. No free lunch theorems for optimization. *IEEE Transactions on Evolutionary Computation*, 1(1):67–82, 1997. doi:10.1109/4235.585893.

- [2] F. F. Assaad. Phase diagram of the half-filled two-dimensional $SU(n)$ hubbard-heisenberg model: A quantum monte carlo study. *Phys. Rev. B*, 71:075103, Feb 2005. doi:10.1103/PhysRevB.71.075103. URL <https://link.aps.org/doi/10.1103/PhysRevB.71.075103>.
- [3] Michael Hermele, T. Senthil, and Matthew P. A. Fisher. Algebraic spin liquid as the mother of many competing orders. *Phys. Rev. B*, 72:104404, Sep 2005. doi:10.1103/PhysRevB.72.104404. URL <https://link.aps.org/doi/10.1103/PhysRevB.72.104404>.
- [4] Hong Yao, Shou-Cheng Zhang, and Steven A. Kivelson. Algebraic spin liquid in an exactly solvable spin model. *Phys. Rev. Lett.*, 102:217202, May 2009. doi:10.1103/PhysRevLett.102.217202. URL <https://link.aps.org/doi/10.1103/PhysRevLett.102.217202>.
- [5] Michael Hermele, Victor Gurarie, and Ana Maria Rey. Mott insulators of ultracold fermionic alkaline earth atoms: Underconstrained magnetism and chiral spin liquid. *Phys. Rev. Lett.*, 103:135301, Sep 2009. doi:10.1103/PhysRevLett.103.135301. URL <https://link.aps.org/doi/10.1103/PhysRevLett.103.135301>.
- [6] Yuan Da Liao, Xiao Yan Xu, Zi Yang Meng, and Yang Qi. Dirac fermions with plaquette interactions. ii. $su(4)$ phase diagram with gross-neveu criticality and quantum spin liquid. *Phys. Rev. B*, 106:115149, Sep 2022. doi:10.1103/PhysRevB.106.115149. URL <https://link.aps.org/doi/10.1103/PhysRevB.106.115149>.
- [7] Xue-Jia Yu, Shao-Hang Shi, Limei Xu, and Zi-Xiang Li. Emergence of competing orders and possible quantum spin liquid in $SU(n)$ fermions. *Phys. Rev. Lett.*, 132:036704, Jan 2024. doi:10.1103/PhysRevLett.132.036704. URL <https://link.aps.org/doi/10.1103/PhysRevLett.132.036704>.
- [8] Carsten Honerkamp and Walter Hofstetter. Ultracold fermions and the $SU(n)$ hubbard model. *Phys. Rev. Lett.*, 92:170403, Apr 2004. doi:10.1103/PhysRevLett.92.170403. URL <https://link.aps.org/doi/10.1103/PhysRevLett.92.170403>.
- [9] Ákos Rapp, Gergely Zaránd, Carsten Honerkamp, and Walter Hofstetter. Color superfluidity and “baryon” formation in ultracold fermions. *Phys. Rev. Lett.*, 98:160405, Apr 2007. doi:10.1103/PhysRevLett.98.160405. URL <https://link.aps.org/doi/10.1103/PhysRevLett.98.160405>.
- [10] Ákos Rapp, Walter Hofstetter, and Gergely Zaránd. Trionic phase of ultracold fermions in an optical lattice: A variational study. *Phys. Rev. B*, 77:144520, Apr 2008. doi:10.1103/PhysRevB.77.144520. URL <https://link.aps.org/doi/10.1103/PhysRevB.77.144520>.
- [11] J. Pohlmann, A. Privitera, I. Titvinidze, and W. Hofstetter. Trion and dimer formation in three-color fermions. *Phys. Rev. A*, 87:023617, Feb 2013. doi:10.1103/PhysRevA.87.023617. URL <https://link.aps.org/doi/10.1103/PhysRevA.87.023617>.
- [12] Han Xu, Xiang Li, Zhichao Zhou, Xin Wang, Lei Wang, Congjun Wu, and Yu Wang. Trion states and quantum criticality of attractive $su(3)$ dirac fermions. *Phys. Rev. Res.*, 5:023180, Jun 2023. doi:10.1103/PhysRevResearch.5.023180. URL <https://link.aps.org/doi/10.1103/PhysRevResearch.5.023180>.
- [13] P. Lecheminant, E. Boulat, and P. Azaria. Confinement and superfluidity in one-dimensional degenerate fermionic cold atoms. *Phys. Rev. Lett.*, 95:240402, Dec 2005. doi:10.1103/PhysRevLett.95.240402. URL <https://link.aps.org/doi/10.1103/PhysRevLett.95.240402>.
- [14] Congjun Wu. Competing orders in one-dimensional spin-3/2 fermionic systems. *Phys. Rev. Lett.*, 95:266404, Dec 2005. doi:10.1103/PhysRevLett.95.266404. URL <https://link.aps.org/doi/10.1103/PhysRevLett.95.266404>.
- [15] Hironobu Yoshida and Hoshio Katsura. Exact eigenstates of extended $SU(n)$ hubbard models: Generalization of η -pairing states with n -particle off-diagonal long-range order. *Phys. Rev. B*, 105:024520, Jan 2022. doi:10.1103/PhysRevB.105.024520. URL <https://link.aps.org/doi/10.1103/PhysRevB.105.024520>.
- [16] Masaya Nakagawa, Hoshio Katsura, and Masahito Ueda. Exact eigenstates of multicomponent hubbard models: $Su(n)$ magnetic η pairing, weak ergodicity breaking, and partial integrability. *Phys. Rev. Res.*, 6:043259, Dec 2024. doi:10.1103/PhysRevResearch.6.043259. URL <https://link.aps.org/doi/10.1103/PhysRevResearch.6.043259>.
- [17] Shohei Imai and Naoto Tsuji. Quantum many-body scars with unconventional superconducting pairing symmetries via multibody interactions. *Phys. Rev. Res.*, 7:013064, Jan 2025. doi:10.1103/PhysRevResearch.7.013064. URL <https://link.aps.org/doi/10.1103/PhysRevResearch.7.013064>.
- [18] Yuan Cao, Valla Fatemi, Shiang Fang, Kenji Watanabe, Takashi Taniguchi, Efthimios Kaxiras, and Pablo Jarillo-Herrero. Unconventional superconductivity in magic-angle graphene superlattices. *Nature*, 556(7699):43–50, April 2018. ISSN 1476-4687. doi:10.1038/nature26160. URL <https://doi.org/10.1038/nature26160>.
- [19] Yuan Cao, Valla Fatemi, Ahmet Demir, Shiang Fang, Spencer L. Tomarken, Jason Y. Luo, Javier D. Sanchez-Yamagishi, Kenji Watanabe, Takashi Taniguchi, Efthimios Kaxiras, Ray C. Ashoori, and Pablo Jarillo-Herrero. Correlated insulator behaviour at half-filling in magic-angle graphene superlattices. *Nature*, 556(7699):80–84, April 2018. ISSN 1476-4687. doi:10.1038/nature26154. URL <https://doi.org/10.1038/nature26154>.
- [20] Cenke Xu and Leon Balents. Topological superconductivity in twisted multilayer graphene. *Phys. Rev. Lett.*, 121:087001, Aug 2018. doi:10.1103/PhysRevLett.121.087001. URL <https://link.aps.org/doi/10.1103/PhysRevLett.121.087001>.
- [21] Dmitry V. Chichinadze, Laura Classen, Yuxuan Wang, and Andrey V. Chubukov. $Su(4)$ symmetry in twisted bilayer graphene: An itinerant perspective. *Phys. Rev. Lett.*, 128:227601, Jun 2022. doi:10.1103/PhysRevLett.128.227601. URL <https://link.aps.org/doi/10.1103/PhysRevLett.128.227601>.
- [22] Nikolaos Parthenios and Laura Classen. Twisted bilayer graphene at charge neutrality: Competing orders of $su(4)$ dirac fermions. *Phys. Rev. B*, 108:235120, Dec 2023. doi:10.1103/PhysRevB.108.235120. URL <https://link.aps.org/doi/10.1103/PhysRevB.108.235120>.
- [23] Cheng Huang, Nikolaos Parthenios, Maksim Ulybyshev, Xu Zhang, Fakher F. Assaad, Laura Classen, and Zi Yang Meng. Angle-tuned Gross-Neveu quantum criticality in twisted bilayer graphene. *Nature Communications*, 16(1):7176, August

2025. ISSN 2041-1723. doi:10.1038/s41467-025-62461-y. URL <https://doi.org/10.1038/s41467-025-62461-y>.
- [24] Eduardo Ibarra-García-Padilla and Sayan Choudhury. Many-body physics of ultracold alkaline-earth atoms with su(n)-symmetric interactions. *Journal of Physics: Condensed Matter*, 37(8):083003, dec 2024. doi:10.1088/1361-648X/ad9658. URL <https://dx.doi.org/10.1088/1361-648X/ad9658>.
- [25] Yasufumi Yamashita, Naokazu Shibata, and Kazuo Ueda. SU(4) spin-orbit critical state in one dimension. *Phys. Rev. B*, 58(14):9114, 1998.
- [26] Roland Assaraf, Patrick Azaria, Michel Caffarel, and Philippe Lecheminant. Metal-insulator transition in the one-dimensional SU(N) Hubbard model. *Phys. Rev. B*, 60(4):2299, 1999.
- [27] M A Cazalilla, A F Ho, and M Ueda. Ultracold gases of ytterbium: Ferromagnetism and Mott states in an SU(6) Fermi system. *New J. Phys.*, 11:103033, 2009. doi:10.1088/1367-2630/11/10/103033.
- [28] Tamás A. Tóth, Andreas M. Läuchli, Frédéric Mila, and Karlo Penc. Three-sublattice ordering of the su(3) heisenberg model of three-flavor fermions on the square and cubic lattices. *Phys. Rev. Lett.*, 105:265301, Dec 2010. doi:10.1103/PhysRevLett.105.265301. URL <https://link.aps.org/doi/10.1103/PhysRevLett.105.265301>.
- [29] Philippe Corboz, Andreas M. Läuchli, Karlo Penc, Matthias Troyer, and Frédéric Mila. Simultaneous dimerization and su(4) symmetry breaking of 4-color fermions on the square lattice. *Phys. Rev. Lett.*, 107:215301, Nov 2011. doi:10.1103/PhysRevLett.107.215301. URL <https://link.aps.org/doi/10.1103/PhysRevLett.107.215301>.
- [30] Salvatore R. Manmana, Kaden R. A. Hazzard, Gang Chen, Adrian E. Feiguin, and Ana Maria Rey. SU(N) magnetism in chains of ultracold alkaline-earth-metal atoms: Mott transitions and quantum correlations. *Phys. Rev. A*, 84:043601, Oct 2011. doi:10.1103/PhysRevA.84.043601. URL <https://link.aps.org/doi/10.1103/PhysRevA.84.043601>.
- [31] Kaden R. A. Hazzard, Victor Gurarie, Michael Hermele, and Ana Maria Rey. High-temperature properties of fermionic alkaline-earth-metal atoms in optical lattices. *Phys. Rev. A*, 85:041604, 2012. doi:10.1103/PhysRevA.85.041604.
- [32] Lars Bonnes, Kaden R. A. Hazzard, Salvatore R. Manmana, Ana Maria Rey, and Stefan Wessel. Adiabatic loading of one-dimensional SU(N) alkaline-earth-atom fermions in optical lattices. *Phys. Rev. Lett.*, 109:205305, Nov 2012. doi:10.1103/PhysRevLett.109.205305. URL <https://link.aps.org/doi/10.1103/PhysRevLett.109.205305>.
- [33] Philippe Corboz, Miklós Lajkó, Andreas M. Läuchli, Karlo Penc, and Frédéric Mila. Spin-orbital quantum liquid on the honeycomb lattice. *Phys. Rev. X*, 2:041013, Nov 2012. doi:10.1103/PhysRevX.2.041013. URL <https://link.aps.org/doi/10.1103/PhysRevX.2.041013>.
- [34] Da Wang, Yi Li, Zi Cai, Zhichao Zhou, Yu Wang, and Congjun Wu. Competing orders in the 2d half-filled SU(2n) hubbard model through the pinning-field quantum monte carlo simulations. *Phys. Rev. Lett.*, 112:156403, Apr 2014. doi:10.1103/PhysRevLett.112.156403. URL <https://link.aps.org/doi/10.1103/PhysRevLett.112.156403>.
- [35] Pierre Nataf and Frédéric Mila. Exact diagonalization of heisenberg SU(n) models. *Phys. Rev. Lett.*, 113:127204, Sep 2014. doi:10.1103/PhysRevLett.113.127204. URL <https://link.aps.org/doi/10.1103/PhysRevLett.113.127204>.
- [36] Shenglong Xu, Julio T. Barreiro, Yu Wang, and Congjun Wu. Interaction effects with varying n in SU(n) symmetric fermion lattice systems. *Phys. Rev. Lett.*, 121:167205, Oct 2018. doi:10.1103/PhysRevLett.121.167205. URL <https://link.aps.org/doi/10.1103/PhysRevLett.121.167205>.
- [37] Daisuke Yamamoto, Chihiro Suzuki, Giacomo Marmorini, Sho Okazaki, and Nobuo Furukawa. Quantum and thermal phase transitions of the triangular su(3) heisenberg model under magnetic fields. *Phys. Rev. Lett.*, 125:057204, Jul 2020. doi:10.1103/PhysRevLett.125.057204. URL <https://link.aps.org/doi/10.1103/PhysRevLett.125.057204>.
- [38] Henning Schrömer, Fabian Grusdt, Ulrich Schollwöck, Kaden R. A. Hazzard, and Annabelle Bohrdt. Subdimensional magnetic polarons in the one-hole doped su(3) $t-j$ model. *Phys. Rev. B*, 110:125134, Sep 2024. doi:10.1103/PhysRevB.110.125134. URL <https://link.aps.org/doi/10.1103/PhysRevB.110.125134>.
- [39] Thomas Botzung and Pierre Nataf. Exact diagonalization of SU(N) Fermi-Hubbard models. *Phys. Rev. Lett.*, 132:153001, Apr 2024. doi:10.1103/PhysRevLett.132.153001. URL <https://link.aps.org/doi/10.1103/PhysRevLett.132.153001>.
- [40] K Buchta, Ö Legeza, E Szirmai, and J Sólyom. Mott transition and dimerization in the one-dimensional SU(N) Hubbard model. *Phys. Rev. B*, 75(15):155108, 2007.
- [41] E. V. Gorelik and N. Blümer. Mott transitions in ternary flavor mixtures of ultracold fermions on optical lattices. *Phys. Rev. A*, 80:051602, Nov 2009. doi:10.1103/PhysRevA.80.051602. URL <https://link.aps.org/doi/10.1103/PhysRevA.80.051602>.
- [42] I Titvinidze, A Privitera, S-Y Chang, S Diehl, M A Baranov, A Daley, and W Hofstetter. Magnetism and domain formation in SU(3)-symmetric multi-species Fermi mixtures. *New J. Phys.*, 13:035013, 2011.
- [43] Andrii Sotnikov and Walter Hofstetter. Magnetic ordering of three-component ultracold fermionic mixtures in optical lattices. *Phys. Rev. A*, 89:063601, Jun 2014. doi:10.1103/PhysRevA.89.063601. URL <https://link.aps.org/doi/10.1103/PhysRevA.89.063601>.
- [44] Zhichao Zhou, Zi Cai, Congjun Wu, and Yu Wang. Quantum Monte Carlo simulations of thermodynamic properties of SU(2N) ultracold fermions in optical lattices. *Phys. Rev. B*, 90(23), dec 2014.
- [45] Andrii Sotnikov. Critical entropies and magnetic-phase-diagram analysis of ultracold three-component fermionic mixtures in optical lattices. *Phys. Rev. A*, 92:023633, Aug 2015. doi:10.1103/PhysRevA.92.023633. URL <https://link.aps.org/doi/10.1103/PhysRevA.92.023633>.
- [46] Gang Chen, Kaden R. A. Hazzard, Ana Maria Rey, and Michael Hermele. Synthetic-gauge-field stabilization of the chiral-spin-liquid phase. *Phys. Rev. A*, 93:061601, Jun 2016. doi:10.1103/PhysRevA.93.061601. URL <https://link.aps.org/doi/10.1103/PhysRevA.93.061601>.
- [47] Zhichao Zhou, Da Wang, Zi Yang Meng, Yu Wang, and Congjun Wu. Mott insulating states and quantum phase transitions of correlated SU(2N) Dirac fermions. *Physical Review B*, 93(24):245157, June 2016. ISSN 2469-9950, 2469-

9969. doi:10.1103/PhysRevB.93.245157. arXiv:1512.03994 [cond-mat].
- [48] Hiromasa Yanatori and Akihisa Koga. Finite-temperature phase transitions in the $SU(N)$ Hubbard model. *Phys. Rev. B*, 94:041110, Jul 2016. doi:10.1103/PhysRevB.94.041110. URL <https://link.aps.org/doi/10.1103/PhysRevB.94.041110>.
- [49] Wenxing Nie, Deping Zhang, and Wei Zhang. Ferromagnetic ground state of the $SU(3)$ Hubbard model on the Lieb lattice. *Phys. Rev. A*, 96(5):053616, 2017.
- [50] Zhichao Zhou, Da Wang, Congjun Wu, and Yu Wang. Finite-temperature valence-bond-solid transitions and thermodynamic properties of interacting $SU(2N)$ Dirac fermions. *Phys. Rev. B*, 95:085128, Feb 2017. doi:10.1103/PhysRevB.95.085128. URL <https://link.aps.org/doi/10.1103/PhysRevB.95.085128>.
- [51] A. Golubeva, A. Sotnikov, A. Cichy, J. Kuneš, and W. Hofstetter. Breaking of $SU(4)$ symmetry and interplay between strongly correlated phases in the Hubbard model. *Phys. Rev. B*, 95:125108, Mar 2017. doi:10.1103/PhysRevB.95.125108. URL <https://link.aps.org/doi/10.1103/PhysRevB.95.125108>.
- [52] Zhichao Zhou, Congjun Wu, and Yu Wang. Mott transition in the π -flux $su(4)$ hubbard model on a square lattice. *Phys. Rev. B*, 97:195122, May 2018. doi:10.1103/PhysRevB.97.195122. URL <https://link.aps.org/doi/10.1103/PhysRevB.97.195122>.
- [53] Mohsen Hafez-Torbati and Walter Hofstetter. Artificial $SU(3)$ spin-orbit coupling and exotic Mott insulators. *Phys. Rev. B*, 98:245131, Dec 2018. doi:10.1103/PhysRevB.98.245131. URL <https://link.aps.org/doi/10.1103/PhysRevB.98.245131>.
- [54] Seung-Sup B. Lee, Jan von Delft, and Andreas Weichselbaum. Filling-driven Mott transition in $SU(N)$ Hubbard models. *Phys. Rev. B*, 97:165143, Apr 2018. doi:10.1103/PhysRevB.97.165143. URL <https://link.aps.org/doi/10.1103/PhysRevB.97.165143>.
- [55] Da Wang, Lei Wang, and Congjun Wu. Slater and mott insulating states in the $su(6)$ hubbard model. *Phys. Rev. B*, 100: 115155, Sep 2019. doi:10.1103/PhysRevB.100.115155. URL <https://link.aps.org/doi/10.1103/PhysRevB.100.115155>.
- [56] Mohsen Hafez-Torbati and Walter Hofstetter. Competing charge and magnetic order in fermionic multicomponent systems. *Phys. Rev. B*, 100:035133, Jul 2019. doi:10.1103/PhysRevB.100.035133. URL <https://link.aps.org/doi/10.1103/PhysRevB.100.035133>.
- [57] Mohsen Hafez-Torbati, Jun-Hui Zheng, Bernhard Irsigler, and Walter Hofstetter. Interaction-driven topological phase transitions in fermionic $SU(3)$ systems. *Phys. Rev. B*, 101:245159, Jun 2020. doi:10.1103/PhysRevB.101.245159. URL <https://link.aps.org/doi/10.1103/PhysRevB.101.245159>.
- [58] A. Pérez-Romero, R. Franco, and J. Silva-Valencia. Phase diagram of the $SU(3)$ Fermi Hubbard model with next-neighbor interactions. *Euro Phys J B*, 94(11):229, nov 2021.
- [59] Eduardo Ibarra-García-Padilla, Sohail Dasgupta, Hao-Tian Wei, Shintaro Taie, Yoshiro Takahashi, Richard T. Scalettar, and Kaden R. A. Hazzard. Universal thermodynamics of an $SU(N)$ Fermi-Hubbard model. *Phys. Rev. A*, 104:043316, Oct 2021. doi:10.1103/PhysRevA.104.043316. URL <https://link.aps.org/doi/10.1103/PhysRevA.104.043316>.
- [60] Vladyslav Unukovich and Andrii Sotnikov. $SU(4)$ -symmetric Hubbard model at quarter filling: Insights from the dynamical mean-field approach. *Phys. Rev. B*, 104:245106, Dec 2021. doi:10.1103/PhysRevB.104.245106. URL <https://link.aps.org/doi/10.1103/PhysRevB.104.245106>.
- [61] Yunqing Ouyang and Xiao Yan Xu. Projection of infinite- U Hubbard model and algebraic sign structure. *Phys. Rev. B*, 104:L241104, Dec 2021. doi:10.1103/PhysRevB.104.L241104. URL <https://link.aps.org/doi/10.1103/PhysRevB.104.L241104>.
- [62] Rajiv R. P. Singh and Jaan Oitmaa. Divergence of magnetic susceptibility in the $SU(N)$ Nagaoka-Thouless ferromagnet. *Phys. Rev. B*, 106:014424, Jul 2022. doi:10.1103/PhysRevB.106.014424. URL <https://link.aps.org/doi/10.1103/PhysRevB.106.014424>.
- [63] Rahul Hingorani, Jaan Oitmaa, and Rajiv R. P. Singh. Onset of charge incompressibility and Mott gaps in the honeycomb-lattice $SU(4)$ Hubbard model: Lessons for twisted bilayer graphene systems. *Phys. Rev. B*, 105:L241410, Jun 2022. doi:10.1103/PhysRevB.105.L241410. URL <https://link.aps.org/doi/10.1103/PhysRevB.105.L241410>.
- [64] Rajiv R. P. Singh and Jaan Oitmaa. Finite-temperature strong-coupling expansions for the $SU(N)$ Hubbard model. *Phys. Rev. A*, 105:033317, Mar 2022. doi:10.1103/PhysRevA.105.033317. URL <https://link.aps.org/doi/10.1103/PhysRevA.105.033317>.
- [65] Eduardo Ibarra-García-Padilla, Chunhan Feng, Giulio Pasqualetti, Simon Fölling, Richard T. Scalettar, Ehsan Khatami, and Kaden R. A. Hazzard. Metal-insulator transition and magnetism of $su(3)$ fermions in the square lattice. *Phys. Rev. A*, 108:053312, Nov 2023. doi:10.1103/PhysRevA.108.053312. URL <https://link.aps.org/doi/10.1103/PhysRevA.108.053312>.
- [66] Chunhan Feng, Eduardo Ibarra-García-Padilla, Kaden R. A. Hazzard, Richard Scalettar, Shiwei Zhang, and Ettore Vitali. Metal-insulator transition and quantum magnetism in the $su(3)$ fermi-hubbard model. *Phys. Rev. Res.*, 5:043267, Dec 2023. doi:10.1103/PhysRevResearch.5.043267. URL <https://link.aps.org/doi/10.1103/PhysRevResearch.5.043267>.
- [67] Mathias Mikkelsen and Ippei Danshita. Relation between the noise correlations and the spin structure factor for Mott-insulating states in $SU(N)$ Hubbard models. *Phys. Rev. A*, 107:043313, Apr 2023. doi:10.1103/PhysRevA.107.043313. URL <https://link.aps.org/doi/10.1103/PhysRevA.107.043313>.
- [68] Han Xu, Yu Wang, Zhichao Zhou, and Congjun Wu. Mott insulating states of the anisotropic $SU(4)$ Dirac fermions. *Physical Review B*, 109(12):125136, March 2024. ISSN 2469-9950, 2469-9969. doi:10.1103/PhysRevB.109.125136. arXiv:1912.11791 [cond-mat].
- [69] Evgeny Kozik. Combinatorial summation of Feynman diagrams: Equation of state of the 2D $SU(N)$ Hubbard model. arXiv:2309.13774, 2024.
- [70] Thomas Botzung and Pierre Nataf. Numerical observation of $SU(N)$ Nagaoka ferromagnetism. *Phys. Rev. B*, 109:235131,

- Jun 2024. doi:10.1103/PhysRevB.109.235131. URL <https://link.aps.org/doi/10.1103/PhysRevB.109.235131>.
- [71] Zewen Zhang, Qinyuan Zheng, Eduardo Ibarra-Garcia-Padilla, Richard T. Scalettar, and Kaden R. A. Hazzard. Unit-density su(3) fermi-hubbard model with spin flavor imbalance, 2025. URL <https://arxiv.org/abs/2503.17776>.
- [72] Samuel Bird, Sebastian Huber, and Jannes Nys. Partial suppression of magnetism in the square lattice su(3) hubbard model, 2025. URL <https://arxiv.org/abs/2507.08073>.
- [73] A. H. Castro Neto, F. Guinea, N. M. R. Peres, K. S. Novoselov, and A. K. Geim. The electronic properties of graphene. *Rev. Mod. Phys.*, 81:109–162, Jan 2009. doi:10.1103/RevModPhys.81.109. URL <https://link.aps.org/doi/10.1103/RevModPhys.81.109>.
- [74] M. Z. Hasan and C. L. Kane. Colloquium: Topological insulators. *Rev. Mod. Phys.*, 82:3045–3067, Nov 2010. doi:10.1103/RevModPhys.82.3045. URL <https://link.aps.org/doi/10.1103/RevModPhys.82.3045>.
- [75] Xiao-Liang Qi and Shou-Cheng Zhang. Topological insulators and superconductors. *Rev. Mod. Phys.*, 83:1057–1110, Oct 2011. doi:10.1103/RevModPhys.83.1057. URL <https://link.aps.org/doi/10.1103/RevModPhys.83.1057>.
- [76] David J. Gross and André Neveu. Dynamical symmetry breaking in asymptotically free field theories. *Phys. Rev. D*, 10: 3235–3253, Nov 1974. doi:10.1103/PhysRevD.10.3235. URL <https://link.aps.org/doi/10.1103/PhysRevD.10.3235>.
- [77] B. Rosenstein, Hoi-Lai Yu, and A. Kovner. Critical exponents of new universality classes. *Phys. Lett. B*, 314(3):381–386, 1993. ISSN 0370-2693. doi:[https://doi.org/10.1016/0370-2693\(93\)91253-J](https://doi.org/10.1016/0370-2693(93)91253-J). URL <https://www.sciencedirect.com/science/article/pii/037026939391253J>.
- [78] Fakher F. Assaad and Igor F. Herbut. Pinning the order: The nature of quantum criticality in the hubbard model on honeycomb lattice. *Phys. Rev. X*, 3:031010, Aug 2013. doi:10.1103/PhysRevX.3.031010. URL <https://link.aps.org/doi/10.1103/PhysRevX.3.031010>.
- [79] Yuichi Otsuka, Seiji Yunoki, and Sandro Sorella. Universal quantum criticality in the metal-insulator transition of two-dimensional interacting dirac electrons. *Phys. Rev. X*, 6:011029, Mar 2016. doi:10.1103/PhysRevX.6.011029. URL <https://link.aps.org/doi/10.1103/PhysRevX.6.011029>.
- [80] Thomas C. Lang, Zi Yang Meng, Alejandro Muramatsu, Stefan Wessel, and Fakher F. Assaad. Dimerized solids and resonating plaquette order in SU(N)-Dirac fermions. *Physical Review Letters*, 111(6):066401, August 2013. ISSN 0031-9007, 1079-7714. doi:10.1103/PhysRevLett.111.066401. arXiv:1306.3258 [cond-mat].
- [81] Francesco Parisen Toldin, Martin Hohenadler, Fakher F. Assaad, and Igor F. Herbut. Fermionic quantum criticality in honeycomb and π -flux hubbard models: Finite-size scaling of renormalization-group-invariant observables from quantum monte carlo. *Phys. Rev. B*, 91:165108, Apr 2015. doi:10.1103/PhysRevB.91.165108. URL <https://link.aps.org/doi/10.1103/PhysRevB.91.165108>.
- [82] Zi-Xiang Li, Yi-Fan Jiang, and Hong Yao. Fermion-sign-free Majorana-quantum-Monte-Carlo studies of quantum critical phenomena of Dirac fermions in two dimensions. *New Journal of Physics*, 17(8):085003, August 2015. ISSN 1367-2630. doi:10.1088/1367-2630/17/8/085003.
- [83] Emilie Huffman and Shailesh Chandrasekharan. Fermion bag approach to hamiltonian lattice field theories in continuous time. *Phys. Rev. D*, 96:114502, Dec 2017. doi:10.1103/PhysRevD.96.114502. URL <https://link.aps.org/doi/10.1103/PhysRevD.96.114502>.
- [84] Ho-Kin Tang, J. N. Leaw, J. N. B. Rodrigues, I. F. Herbut, P. Sengupta, F. F. Assaad, and S. Adam. The role of electron-electron interactions in two-dimensional dirac fermions. *Science*, 361(6402):570–574, 2018. doi:10.1126/science.aao2934. URL <https://www.science.org/doi/abs/10.1126/science.aao2934>.
- [85] Pavel Buividovich, Dominik Smith, Maksim Ulybyshev, and Lorenz von Smekal. Hybrid monte carlo study of competing order in the extended fermionic hubbard model on the hexagonal lattice. *Phys. Rev. B*, 98:235129, Dec 2018. doi:10.1103/PhysRevB.98.235129. URL <https://link.aps.org/doi/10.1103/PhysRevB.98.235129>.
- [86] Xiao Yan Xu and Tarun Grover. Competing nodal d -wave superconductivity and antiferromagnetism. *Phys. Rev. Lett.*, 126:217002, May 2021. doi:10.1103/PhysRevLett.126.217002. URL <https://link.aps.org/doi/10.1103/PhysRevLett.126.217002>.
- [87] Thomas C. Lang and Andreas M. Läuchli. Chiral heisenberg gross-neveu-yukawa criticality: honeycomb vs. slac fermions, 2025. URL <https://arxiv.org/abs/2503.15000>.
- [88] Lukas Janssen and Igor F. Herbut. Antiferromagnetic critical point on graphene’s honeycomb lattice: A functional renormalization group approach. *Phys. Rev. B*, 89:205403, May 2014. doi:10.1103/PhysRevB.89.205403. URL <https://link.aps.org/doi/10.1103/PhysRevB.89.205403>.
- [89] Benjamin Knorr. Ising and gross-neveu model in next-to-leading order. *Phys. Rev. B*, 94:245102, Dec 2016. doi:10.1103/PhysRevB.94.245102. URL <https://link.aps.org/doi/10.1103/PhysRevB.94.245102>.
- [90] Nikolai Zerf, Luminita N. Mihaila, Peter Marquard, Igor F. Herbut, and Michael M. Scherer. Four-loop critical exponents for the gross-neveu-yukawa models. *Phys. Rev. D*, 96:096010, Nov 2017. doi:10.1103/PhysRevD.96.096010. URL <https://link.aps.org/doi/10.1103/PhysRevD.96.096010>.
- [91] Bernhard Ihrig, Luminita N. Mihaila, and Michael M. Scherer. Critical behavior of dirac fermions from perturbative renormalization. *Phys. Rev. B*, 98:125109, Sep 2018. doi:10.1103/PhysRevB.98.125109. URL <https://link.aps.org/doi/10.1103/PhysRevB.98.125109>.
- [92] J. A. Gracey. Large n critical exponents for the chiral heisenberg gross-neveu universality class. *Phys. Rev. D*, 97:105009, May 2018. doi:10.1103/PhysRevD.97.105009. URL <https://link.aps.org/doi/10.1103/PhysRevD.97.105009>.
- [93] Benjamin Knorr. Critical chiral heisenberg model with the functional renormalization group. *Phys. Rev. B*, 97:075129, Feb 2018. doi:10.1103/PhysRevB.97.075129. URL <https://link.aps.org/doi/10.1103/PhysRevB.97.075129>.
- [94] N. Read and Subir Sachdev. Valence-bond and spin-peierls ground states of low-dimensional quantum antiferromagnets. *Phys. Rev. Lett.*, 62:1694–1697, Apr 1989. doi:10.1103/PhysRevLett.62.1694. URL <https://link.aps.org/doi/10.1103/PhysRevLett.62.1694>.

- [1103/PhysRevLett.62.1694](https://doi.org/10.1103/PhysRevLett.62.1694).
- [95] N. Read and Subir Sachdev. Spin-peierls, valence-bond solid, and néel ground states of low-dimensional quantum antiferromagnets. *Phys. Rev. B*, 42:4568–4589, Sep 1990. doi:10.1103/PhysRevB.42.4568. URL <https://link.aps.org/doi/10.1103/PhysRevB.42.4568>.
- [96] Xiao Yan Xu, Yang Qi, Long Zhang, Fakher F. Assaad, Cenke Xu, and Zi Yang Meng. Monte carlo study of lattice compact quantum electrodynamics with fermionic matter: The parent state of quantum phases. *Phys. Rev. X*, 9:021022, May 2019. doi:10.1103/PhysRevX.9.021022. URL <https://link.aps.org/doi/10.1103/PhysRevX.9.021022>.
- [97] Wei Wang, Da-Chuan Lu, Xiao Yan Xu, Yi-Zhuang You, and Zi Yang Meng. Dynamics of compact quantum electrodynamics at large fermion flavor. *Phys. Rev. B*, 100:085123, Aug 2019. doi:10.1103/PhysRevB.100.085123. URL <https://link.aps.org/doi/10.1103/PhysRevB.100.085123>.
- [98] Lukas Janssen, Wei Wang, Michael M. Scherer, Zi Yang Meng, and Xiao Yan Xu. Confinement transition in the qed_3 -gross-neveu-xy universality class. *Phys. Rev. B*, 101:235118, Jun 2020. doi:10.1103/PhysRevB.101.235118. URL <https://link.aps.org/doi/10.1103/PhysRevB.101.235118>.
- [99] SangEun Han and Igor F. Herbut. Gross-neveu-yukawa theory of $\text{SO}(2n) \rightarrow \text{SO}(n) \times \text{SO}(n)$ spontaneous symmetry breaking. *Phys. Rev. B*, 110:125131, Sep 2024. doi:10.1103/PhysRevB.110.125131. URL <https://link.aps.org/doi/10.1103/PhysRevB.110.125131>.
- [100] Shouryya Ray. Unconventional gross-neveu quantum criticality: Interaction-induced $\text{so}(3)$ -biadjoint insulator and emergent $\text{su}(3)$ symmetry. *Phys. Rev. B*, 109:165137, Apr 2024. doi:10.1103/PhysRevB.109.165137. URL <https://link.aps.org/doi/10.1103/PhysRevB.109.165137>.
- [101] SangEun Han, Shouryya Ray, and Igor F. Herbut. Gross-neveu-yukawa $\text{so}(2)$ and $\text{so}(3)$ tensorial criticality. *Phys. Rev. B*, 111:115131, Mar 2025. doi:10.1103/PhysRevB.111.115131. URL <https://link.aps.org/doi/10.1103/PhysRevB.111.115131>.
- [102] Shintaro Taie, Rekishu Yamazaki, Seiji Sugawa, and Yoshiro Takahashi. An $\text{SU}(6)$ Mott insulator of an atomic Fermi gas realized by large-spin Pomeranchuk cooling. *Nature Physics*, 8(11):825–830, November 2012. ISSN 1745-2481. doi:10.1038/nphys2430. URL <https://doi.org/10.1038/nphys2430>.
- [103] Christian Hofrichter, Luis Riegger, Francesco Scazza, Moritz Höfer, Diogo Rio Fernandes, Immanuel Bloch, and Simon Fölling. Direct probing of the mott crossover in the $\text{SU}(n)$ fermi-hubbard model. *Phys. Rev. X*, 6:021030, Jun 2016. doi:10.1103/PhysRevX.6.021030. URL <https://link.aps.org/doi/10.1103/PhysRevX.6.021030>.
- [104] Hideki Ozawa, Shintaro Taie, Yosuke Takasu, and Yoshiro Takahashi. Antiferromagnetic spin correlation of $\text{SU}(\mathcal{N})$ fermi gas in an optical superlattice. *Phys. Rev. Lett.*, 121:225303, Nov 2018. doi:10.1103/PhysRevLett.121.225303. URL <https://link.aps.org/doi/10.1103/PhysRevLett.121.225303>.
- [105] Shintaro Taie, Eduardo Ibarra-García-Padilla, Naoki Nishizawa, Yosuke Takasu, Yoshihito Kuno, Hao-Tian Wei, Richard T. Scalettar, Kaden R. A. Hazzard, and Yoshiro Takahashi. Observation of antiferromagnetic correlations in an ultracold $\text{SU}(N)$ Hubbard model. *Nature Physics*, 18(11):1356–1361, November 2022. ISSN 1745-2481. doi:10.1038/s41567-022-01725-6. URL <https://doi.org/10.1038/s41567-022-01725-6>.
- [106] D. Tusi, L. Franchi, L. F. Livi, K. Baumann, D. Benedicto Orenes, L. Del Re, R. E. Barfknecht, T.-W. Zhou, M. Inguscio, G. Cappellini, M. Capone, J. Catani, and L. Fallani. Flavour-selective localization in interacting lattice fermions. *Nature Physics*, 18(10):1201–1205, October 2022. ISSN 1745-2481. doi:10.1038/s41567-022-01726-5. URL <https://doi.org/10.1038/s41567-022-01726-5>.
- [107] G. Pasqualetti, O. Bettermann, N. Darkwah Oppong, E. Ibarra-García-Padilla, S. Dasgupta, R. T. Scalettar, K. R. A. Hazzard, I. Bloch, and S. Fölling. Equation of state and thermometry of the 2d $\text{SU}(n)$ fermi-hubbard model. *Phys. Rev. Lett.*, 132:083401, Feb 2024. doi:10.1103/PhysRevLett.132.083401. URL <https://link.aps.org/doi/10.1103/PhysRevLett.132.083401>.
- [108] Ryuta Yamamoto, Jun Kobayashi, Takuma Kuno, Kohei Kato, and Yoshiro Takahashi. An ytterbium quantum gas microscope with narrow-line laser cooling. *New J. Phys.*, 18(2):023016, feb 2016. doi:10.1088/1367-2630/18/2/023016.
- [109] Daichi Okuno, Yoshiki Amano, Katsunari Enomoto, Nobuyuki Takei, and Yoshiro Takahashi. Schemes for nondestructive quantum gas microscopy of single atoms in an optical lattice. *New J. Phys.*, 22(1):013041, jan 2020. doi:10.1088/1367-2630/ab6af9.
- [110] Sandra Buob, Jonatan Höschele, Vasiliy Makhalov, Antonio Rubio-Abadal, and Leticia Tarruell. A strontium quantum-gas microscope. *PRX Quantum*, 5:020316, Apr 2024. doi:10.1103/PRXQuantum.5.020316. URL <https://link.aps.org/doi/10.1103/PRXQuantum.5.020316>.
- [111] Lin Su, Alexander Douglas, Michal Szurek, Anne H. Hébert, Aaron Krahm, Robin Groth, Gregory A. Phelps, Ognjen Marković, and Markus Greiner. Fast single atom imaging for optical lattice arrays. *Nature Communications*, 16(1), January 2025. ISSN 2041-1723. doi:10.1038/s41467-025-56305-y. URL <http://dx.doi.org/10.1038/s41467-025-56305-y>.
- [112] Aaron Merlin Müller, Miklós Lajkó, Florian Schreck, Frédéric Mila, and Jiří Minář. State selective cooling of $\text{SU}(N)$ Fermi gases. *Phys. Rev. A*, 104:013304, Jul 2021. doi:10.1103/PhysRevA.104.013304. URL <https://link.aps.org/doi/10.1103/PhysRevA.104.013304>.
- [113] Daisuke Yamamoto and Katsuhiro Morita. Engineering of a low-entropy quantum simulator for strongly correlated electrons using cold atoms with $\text{SU}(\mathcal{N})$ -symmetric interactions. *Phys. Rev. Lett.*, 132:213401, May 2024. doi:10.1103/PhysRevLett.132.213401. URL <https://link.aps.org/doi/10.1103/PhysRevLett.132.213401>.
- [114] Rajeev S. Erramilli, Luca V. Iliesiu, Petr Kravchuk, Aike Liu, David Poland, and David Simmons-Duffin. The Gross-Neveu-Yukawa archipelago. *Journal of High Energy Physics*, 2023(2):36, February 2023. ISSN 1029-8479. doi:10.1007/JHEP02(2023)036. URL [https://doi.org/10.1007/JHEP02\(2023\)036](https://doi.org/10.1007/JHEP02(2023)036).
- [115] Mitsutoshi Fujita, René Meyer, Sumiran Pujari, and Masaki Tezuka. Effective hopping in holographic Bose and

- Fermi-Hubbard models. *Journal of High Energy Physics*, 2019(1):45, January 2019. ISSN 1029-8479. doi: 10.1007/JHEP01(2019)045. URL [https://doi.org/10.1007/JHEP01\(2019\)045](https://doi.org/10.1007/JHEP01(2019)045).
- [116] Joshua Erlich, Emanuel Katz, Dam T. Son, and Mikhail A. Stephanov. Qcd and a holographic model of hadrons. *Phys. Rev. Lett.*, 95:261602, Dec 2005. doi:10.1103/PhysRevLett.95.261602. URL <https://link.aps.org/doi/10.1103/PhysRevLett.95.261602>.
- [117] S. Raghu, Xiao-Liang Qi, C. Honerkamp, and Shou-Cheng Zhang. Topological mott insulators. *Phys. Rev. Lett.*, 100: 156401, Apr 2008. doi:10.1103/PhysRevLett.100.156401. URL <https://link.aps.org/doi/10.1103/PhysRevLett.100.156401>.
- [118] C. Weeks and M. Franz. Interaction-driven instabilities of a dirac semimetal. *Phys. Rev. B*, 81:085105, Feb 2010. doi:10.1103/PhysRevB.81.085105. URL <https://link.aps.org/doi/10.1103/PhysRevB.81.085105>.
- [119] Adolfo G. Grushin, Eduardo V. Castro, Alberto Cortijo, Fernando de Juan, María A. H. Vozmediano, and Belén Valenzuela. Charge instabilities and topological phases in the extended hubbard model on the honeycomb lattice with enlarged unit cell. *Phys. Rev. B*, 87:085136, Feb 2013. doi:10.1103/PhysRevB.87.085136. URL <https://link.aps.org/doi/10.1103/PhysRevB.87.085136>.
- [120] Noel A. García-Martínez, Adolfo G. Grushin, Titus Neupert, Belén Valenzuela, and Eduardo V. Castro. Interaction-driven phases in the half-filled spinless honeycomb lattice from exact diagonalization. *Phys. Rev. B*, 88:245123, Dec 2013. doi:10.1103/PhysRevB.88.245123. URL <https://link.aps.org/doi/10.1103/PhysRevB.88.245123>.
- [121] Maria Dagofer and Martin Hohenadler. Phases of correlated spinless fermions on the honeycomb lattice. *Phys. Rev. B*, 89: 035103, Jan 2014. doi:10.1103/PhysRevB.89.035103. URL <https://link.aps.org/doi/10.1103/PhysRevB.89.035103>.
- [122] Sylvain Capponi and Andreas M. Läuchli. Phase diagram of interacting spinless fermions on the honeycomb lattice: A comprehensive exact diagonalization study. *Phys. Rev. B*, 92:085146, Aug 2015. doi:10.1103/PhysRevB.92.085146. URL <https://link.aps.org/doi/10.1103/PhysRevB.92.085146>.
- [123] Johannes Motruk, Adolfo G. Grushin, Fernando de Juan, and Frank Pollmann. Interaction-driven phases in the half-filled honeycomb lattice: An infinite density matrix renormalization group study. *Phys. Rev. B*, 92:085147, Aug 2015. doi:10.1103/PhysRevB.92.085147. URL <https://link.aps.org/doi/10.1103/PhysRevB.92.085147>.
- [124] Daniel D. Scherer, Michael M. Scherer, and Carsten Honerkamp. Correlated spinless fermions on the honeycomb lattice revisited. *Phys. Rev. B*, 92:155137, Oct 2015. doi:10.1103/PhysRevB.92.155137. URL <https://link.aps.org/doi/10.1103/PhysRevB.92.155137>.
- [125] Sylvain Capponi. Phase diagram of interacting spinless fermions on the honeycomb lattice. *Journal of Physics: Condensed Matter*, 29(4):043002, nov 2016. doi:10.1088/1361-648X/29/4/043002. URL <https://dx.doi.org/10.1088/1361-648X/29/4/043002>.
- [126] Stephan Rachel. Interacting topological insulators: a review. *Reports on Progress in Physics*, 81(11):116501, oct 2018. doi:10.1088/1361-6633/aad6a6. URL <https://dx.doi.org/10.1088/1361-6633/aad6a6>.
- [127] Norman Paris, Karim Bouadim, Frederic Hebert, G George Batrouni, and RT Scalettar. Quantum monte carlo study of an interaction-driven band-insulator-to-metal transition. *Physical review letters*, 98(4):046403, 2007.
- [128] R. Mondaini, S. Tarat, and R. T. Scalettar. Quantum critical points and the sign problem. *Science*, 375(6579):418–424, 2022. doi:10.1126/science.abg9299. URL <https://www.science.org/doi/abs/10.1126/science.abg9299>.
- [129] W. M. C. Foulkes, L. Mitas, R. J. Needs, and G. Rajagopal. Quantum monte carlo simulations of solids. *Rev. Mod. Phys.*, 73:33–83, Jan 2001. doi:10.1103/RevModPhys.73.33. URL <https://link.aps.org/doi/10.1103/RevModPhys.73.33>.
- [130] George H. Booth, Andreas Grüneis, Georg Kresse, and Ali Alavi. Towards an exact description of electronic wavefunctions in real solids. *Nature*, 493(7432):365–370, January 2013. ISSN 1476-4687. doi:10.1038/nature11770. URL <https://doi.org/10.1038/nature11770>.
- [131] James J. Shepherd, Gustavo E. Scuseria, and James S. Spencer. Sign problem in full configuration interaction quantum monte carlo: Linear and sublinear representation regimes for the exact wave function. *Phys. Rev. B*, 90:155130, Oct 2014. doi:10.1103/PhysRevB.90.155130. URL <https://link.aps.org/doi/10.1103/PhysRevB.90.155130>.
- [132] Mario Motta and Shiwei Zhang. Ab initio computations of molecular systems by the auxiliary-field quantum monte carlo method. *WIREs Computational Molecular Science*, 8(5):e1364, 2018. doi:<https://doi.org/10.1002/wcms.1364>. URL <https://wires.onlinelibrary.wiley.com/doi/abs/10.1002/wcms.1364>.
- [133] Hayley R. Petras, Sai Kumar Ramadugu, Fionn D. Malone, and James J. Shepherd. Using density matrix quantum monte carlo for calculating exact-on-average energies for ab initio hamiltonians in a finite basis set. *Journal of Chemical Theory and Computation*, 16(2):1029–1038, 2020. doi:10.1021/acs.jctc.9b01080. URL <https://doi.org/10.1021/acs.jctc.9b01080>. PMID: 31944692.
- [134] Hayley R. Petras, William Z. Van Benschoten, Sai Kumar Ramadugu, and James J. Shepherd. The sign problem in density matrix quantum monte carlo. *Journal of Chemical Theory and Computation*, 17(10):6036–6052, 2021. doi: 10.1021/acs.jctc.1c00078. URL <https://doi.org/10.1021/acs.jctc.1c00078>. PMID: 34546738.
- [135] Ankit Mahajan and Sandeep Sharma. Taming the sign problem in auxiliary-field quantum monte carlo using accurate wave functions. *Journal of Chemical Theory and Computation*, 17(8):4786–4798, 2021. doi:10.1021/acs.jctc.1c00371. URL <https://doi.org/10.1021/acs.jctc.1c00371>. PMID: 34232637.
- [136] Joonho Lee, Hung Q. Pham, and David R. Reichman. Twenty years of auxiliary-field quantum monte carlo in quantum chemistry: An overview and assessment on main group chemistry and bond-breaking. *Journal of Chemical Theory and Computation*, 18(12):7024–7042, 2022. doi:10.1021/acs.jctc.2c00802. URL <https://doi.org/10.1021/acs.jctc.2c00802>. PMID: 36255074.
- [137] James Shee, John L. Weber, David R. Reichman, Richard A. Friesner, and Shiwei Zhang. On the potentially transformative role of auxiliary-field quantum Monte Carlo in quantum chemistry: A highly accurate method for

- transition metals and beyond. *The Journal of Chemical Physics*, 158(14):140901, April 2023. ISSN 0021-9606. doi:10.1063/5.0134009. URL <https://doi.org/10.1063/5.0134009>. eprint: https://pubs.aip.org/aip/jcp/article-pdf/doi/10.1063/5.0134009/20004431/140901_1.5.0134009.pdf.
- [138] Weiluo Ren, Weizhong Fu, Xiaojie Wu, and Ji Chen. Towards the ground state of molecules via diffusion Monte Carlo on neural networks. *Nature Communications*, 14(1):1860, April 2023. ISSN 2041-1723. doi:10.1038/s41467-023-37609-3. URL <https://doi.org/10.1038/s41467-023-37609-3>.
- [139] Alfonso Annarelli, Dario Alfè, and Andrea Zen. A brief introduction to the diffusion Monte Carlo method and the fixed-node approximation. *The Journal of Chemical Physics*, 161(24):241501, December 2024. ISSN 0021-9606. doi:10.1063/5.0232424. URL <https://doi.org/10.1063/5.0232424>. eprint: https://pubs.aip.org/aip/jcp/article-pdf/doi/10.1063/5.0232424/20322370/241501_1.5.0232424.pdf.
- [140] R. L. Workman et al. Review of Particle Physics. *PTEP*, 2022:083C01, 2022. doi:10.1093/ptep/ptac097.
- [141] M. A. Stephanov. QCD phase diagram: An Overview. *PoS*, LAT2006:024, 2006. doi:10.22323/1.032.0024.
- [142] Philippe de Forcrand. Simulating QCD at finite density. *PoS*, LAT2009:010, 2009. doi:10.22323/1.091.0010.
- [143] R.A. Soltz, C. DeTar, F. Karsch, Swagato Mukherjee, and P. Vranas. Lattice qcd thermodynamics with physical quark masses. *Annual Review of Nuclear and Particle Science*, 65(Volume 65, 2015):379–402, 2015. ISSN 1545-4134. doi: <https://doi.org/10.1146/annurev-nucl-102014-022157>. URL <https://www.annualreviews.org/content/journals/10.1146/annurev-nucl-102014-022157>.
- [144] Gert Aarts. Introductory lectures on lattice qcd at nonzero baryon number. *Journal of Physics: Conference Series*, 706(2):022004, apr 2016. doi:10.1088/1742-6596/706/2/022004. URL <https://dx.doi.org/10.1088/1742-6596/706/2/022004>.
- [145] D. T. Son and M. A. Stephanov. Dynamic universality class of the qcd critical point. *Phys. Rev. D*, 70:056001, Sep 2004. doi:10.1103/PhysRevD.70.056001. URL <https://link.aps.org/doi/10.1103/PhysRevD.70.056001>.
- [146] Swagato Mukherjee, Raju Venugopalan, and Yi Yin. Universal off-equilibrium scaling of critical cumulants in the qcd phase diagram. *Phys. Rev. Lett.*, 117:222301, Nov 2016. doi:10.1103/PhysRevLett.117.222301. URL <https://link.aps.org/doi/10.1103/PhysRevLett.117.222301>.
- [147] Yukinao Akamatsu, Derek Teaney, Fanglida Yan, and Yi Yin. Transits of the qcd critical point. *Phys. Rev. C*, 100:044901, Oct 2019. doi:10.1103/PhysRevC.100.044901. URL <https://link.aps.org/doi/10.1103/PhysRevC.100.044901>.
- [148] Christian Schmidt. The qcd phase diagram, universal scaling, and lee-yang zeros. *Journal of Subatomic Particles and Cosmology*, 3:100057, 2025. ISSN 3050-4805. doi:<https://doi.org/10.1016/j.jspc.2025.100057>. URL <https://www.sciencedirect.com/science/article/pii/S3050480525000378>.
- [149] Erez Berg, Max A. Metlitski, and Subir Sachdev. Sign-problem-free quantum monte carlo of the onset of antiferromagnetism in metals. *Science*, 338(6114):1606–1609, 2012. doi:10.1126/science.1227769. URL <https://www.science.org/doi/abs/10.1126/science.1227769>.
- [150] Zohar Ringel and Dmitry L. Kovrizhin. Quantized gravitational responses, the sign problem, and quantum complexity. *Science Advances*, 3(9):e1701758, 2017. doi:10.1126/sciadv.1701758. URL <https://www.science.org/doi/abs/10.1126/sciadv.1701758>.
- [151] Dominik Hangleiter, Ingo Roth, Daniel Nagaj, and Jens Eisert. Easing the monte carlo sign problem. *Science Advances*, 6(33):eabb8341, 2020. doi:10.1126/sciadv.eabb8341. URL <https://www.science.org/doi/abs/10.1126/sciadv.eabb8341>.